ANNUAL REVIEWS

Annual Review of Marine Science

The Four-Dimensional Carbon Cycle of the Southern Ocean

Alison R. Gray

School of Oceanography, University of Washington, Seattle, Washington, USA; email: argray@uw.edu

Annu. Rev. Mar. Sci. 2024. 16:163–90

First published as a Review in Advance on September 22, 2023

The *Annual Review of Marine Science* is online at marine.annualreviews.org

https://doi.org/10.1146/annurev-marine-041923-104057

Keywords

Southern Ocean, ocean carbon cycle, overturning circulation, seasonal cycle, zonal asymmetry, mesoscale variability, Southern Hemisphere storms

Abstract

The Southern Ocean plays a fundamental role in the global carbon cycle, dominating the oceanic uptake of heat and carbon added by anthropogenic activities and modulating atmospheric carbon concentrations in past, present, and future climates. However, the remote and extreme conditions found there make the Southern Ocean perpetually one of the most difficult places on the planet to observe and to model, resulting in significant and persistent uncertainties in our knowledge of the oceanic carbon cycle there. The flow of carbon in the Southern Ocean is traditionally understood using a zonal mean framework, in which the meridional overturning circulation drives the latitudinal variability observed in both air–sea flux and interior ocean carbon concentration. However, recent advances, based largely on expanded observation and modeling capabilities in the region, reveal the importance of processes acting at smaller scales, including basin-scale zonal asymmetries in mixed-layer depth, mesoscale eddies, and high-frequency atmospheric variability. Assessing the current state of knowledge and remaining gaps emphasizes the need to move beyond the zonal mean picture and embrace a four-dimensional understanding of the carbon cycle in the Southern Ocean.

1. INTRODUCTION

Located at the intersection of the atmosphere, the cryosphere, the surface ocean, and the deep, the Southern Ocean exerts a unique and outsized impact on the global climate system. Fundamentally, this influence originates with the fact that the Southern Ocean—considered here to be the vast ocean south of 35°S—is the only place on Earth where the ocean can travel around the globe unimpeded by continents (**Figure 1*a*,*b***). Driven by the vigorous westerly winds found at

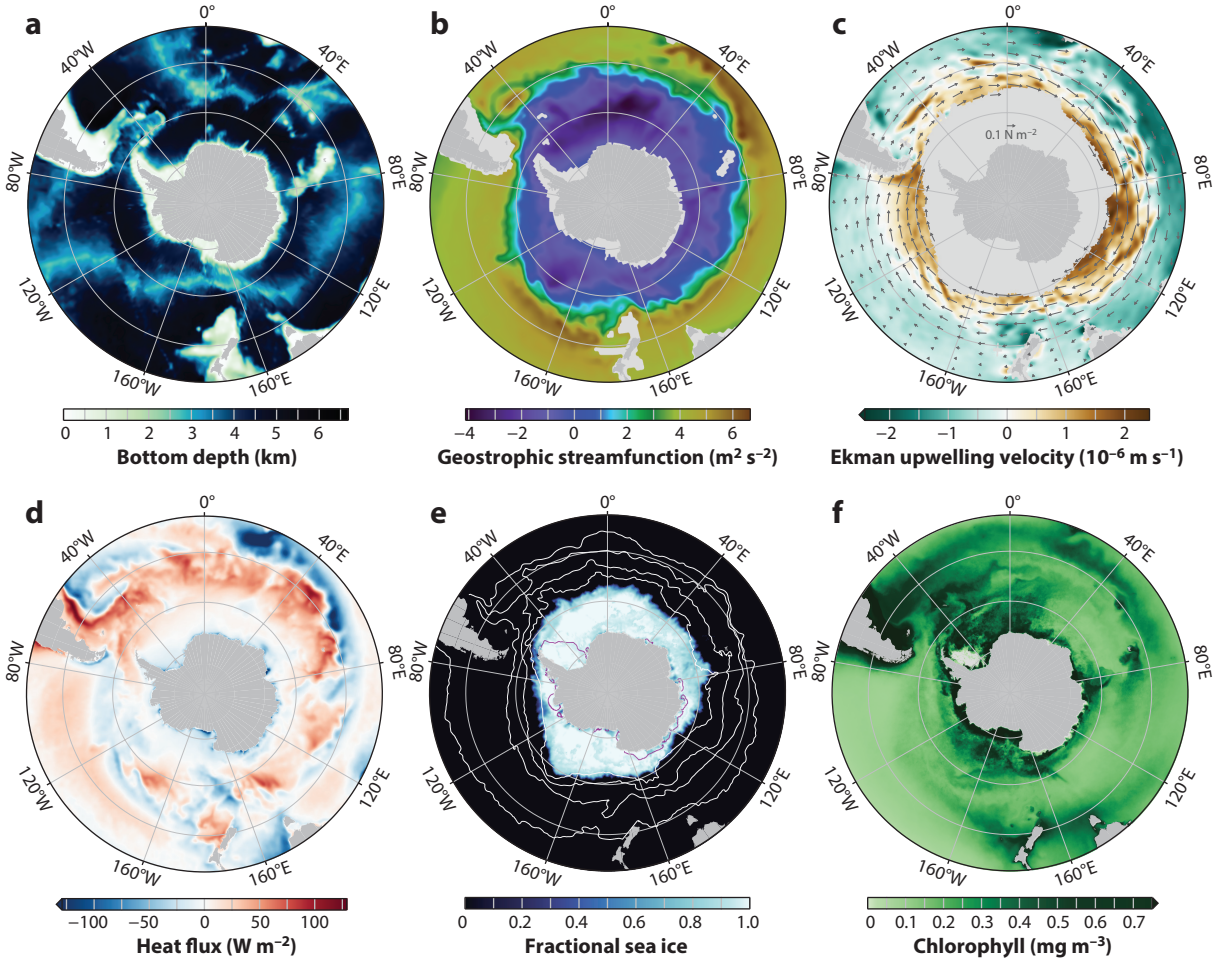

Figure 1

Physical and biological properties in the Southern Ocean. (*a*) Seafloor bathymetry (Amante & Eakins 2009). (*b*) Mean 2001–2020 geostrophic streamfunction at 800–1,200 dbar computed from the Scripps Argo trajectory-based velocity product (Zilberman et al. 2023). (*c*) Mean 1999–2009 surface wind stress (*arrows*) and Ekman upwelling velocity (*colored shading*) computed from the Scatterometer Climatology of Ocean Winds (Risien & Chelton 2008). (*d*) Mean 2001–2020 surface heat flux computed from European Centre for Medium-Range Weather Forecasts Reanalysis 5 (Hersbach et al. 2023), with positive indicating flux into the ocean. (*e*) 2001–2020 maximum and minimum sea ice extent (Meier et al. 2021), where the colored shading shows fractional sea ice cover (f_{ice}) on September 21, 2014, and the pink line shows the $f_{ice} = 0.15$ contour on March 3, 2017. The thin white lines show, from north to south, the Subtropical Front (Gray et al. 2018) and the Sub-Antarctic Front, the Polar Front, and the Southern Antarctic Circumpolar Current Front (Kim & Orsi 2014). (*f*) Mean 2003–2022 surface chlorophyll concentration computed from the Moderate Resolution Imaging Spectroradiometer (NASA Ocean Biol. Process. Group 2022).

midlatitudes (**Figure 1*c***), the Antarctic Circumpolar Current (ACC) transports more water than any other oceanic current as it flows eastward around the planet. The secondary circulation that develops as a result of these dynamics, together with significant air–sea heat fluxes (**Figure 1*d***) and seasonal growth and retreat of an enormous quantity of sea ice (**Figure 1*e***), places the Southern Ocean at the center of the global meridional overturning circulation and the associated ventilation of the deep ocean (Marshall & Speer 2012, Talley 2013).

Through this unique connection to the deep ocean, which constitutes the largest labile reservoir of carbon on Earth (Sarmiento & Gruber 2006), the Southern Ocean has a governing influence on the global carbon cycle and thus on Earth's climate. In the modern era, decadal shifts in the total uptake of carbon dioxide (CO_2) by the global ocean are driven by variability in the Southern Ocean air–sea carbon flux, which is often attributed to changes in the overturning circulation of the Southern Hemisphere (Le Quéré et al. 2007, Landschützer et al. 2015). The Southern Ocean plays a critical role in taking up anthropogenic carbon (C_{ANT}) from the atmosphere (Frölicher et al. 2015) and influences global cycling of organic carbon via the supply of macronutrients to low-latitude surface waters (Sarmiento et al. 2004). Changes to the Southern Ocean carbon cycle were also central to many past climate transitions, with reported impacts ranging from the recent geologic past (Rae et al. 2018, Studer et al. 2018) to epochs that occurred millions of years ago (Ai et al. 2020, Abell et al. 2021). Furthermore, predictions of future change implicate the Southern Ocean in the variability of the global carbon cycle at timescales ranging from interannual (Gallego et al. 2020) to decadal (Li & Ilyina 2018) to multicentennial (Chikamoto & DiNezio 2021).

Despite its clear importance in the global climate system, significant gaps in our knowledge of the Southern Ocean carbon cycle persist. The processes that govern the flow of carbon in this high-latitude region exhibit substantial variability on a wide range of spatiotemporal scales, with particularly strong changes occurring over the seasonal cycle. Shipboard measurements, which are inherently limited in the Southern Ocean—especially in winter—do not constrain the full spectrum of variability in the carbon system, leading to large uncertainties in observation-based estimates (Gloege et al. 2021, Djeutchouang et al. 2022). Air–sea carbon fluxes determined by interpolating sparse shipboard measurements across the entire region diverge substantially from those based on numerical simulations, in both the mean and the variability (Mongwe et al. 2018, Hauck et al. 2020). The overall strength of oceanic carbon uptake in this region is an active area of research, with novel observations recently collected by profiling floats indicating vigorous wintertime outgassing at high latitudes (Gray et al. 2018, Bushinsky et al. 2019a). The associated reductions in the annual net flux were subsequently challenged, however, using aircraft-based measurements of vertical gradients in atmospheric CO_2 and oxygen over the Southern Ocean (Long et al. 2021). Reducing the significant uncertainty in estimates of the oceanic carbon cycle requires making meaningful advances in observing, modeling, and ultimately understanding the flow of carbon through the Southern Ocean across a broad range of spatiotemporal scales.

Recognizing these substantial gaps in our scientific knowledge, investigators have conducted a variety of important research activities in the Southern Ocean over the past decade, immensely expanding our ability to observe and model the physics and biogeochemistry of this region. Consequently, a critical shift has begun in how the meridional overturning circulation of the Southern Ocean is conceptualized, moving beyond the classic, two-dimensional framework that removes longitudinal variation through zonal averaging (Marshall & Speer 2012) to one in which localized and small-scale processes are central (Rintoul 2018, Morrison et al. 2022). At the same time, significant progress has been made in understanding variability in the biologically driven impacts on carbon in the Southern Ocean on a range of spatial and temporal scales (Person et al. 2018, Tréguer et al. 2018, Iversen 2023, Siegel et al. 2023). Yet the Southern Ocean carbon cycle is still

viewed primarily through a zonally averaged lens (Gruber et al. 2019b), which raises several important questions: What is the distribution of carbon in the surface and interior ocean, in three spatial dimensions and at annual, seasonal, and subseasonal timescales? How does spatiotemporal variability in the governing physical and biogeochemical mechanisms regulate the flow of carbon through the coupled ocean–atmosphere–ice system in this critical polar environment? What role do localized and small-scale processes play in modulating changes in the Southern Ocean carbon cycle at larger scales, especially the response to anthropogenic forcing? And how does the four-dimensional variability in this vast and distant ocean impact our ability to measure, understand, and predict the Southern Ocean carbon cycle across a variety of scales?

To help address these questions, this review synthesizes current understanding of the contemporary Southern Ocean carbon cycle, its variability in three dimensions and at annual to subseasonal timescales, and the physical and biogeochemical processes that generate that variability. Although changes occurring on interannual, decadal, or even longer timescales are not explicitly emphasized here, characterizing the substantial variability at shorter spatiotemporal scales provides necessary context for accurately detecting these crucially important longer-term changes, especially in light of traditional sampling biases. This work focuses primarily on knowledge gained from observational approaches, mainly in the open Southern Ocean (including the regions seasonally covered in sea ice) as opposed to coastal areas on the Antarctic shelf. Examination of recent estimates of ocean–atmosphere CO_2 exchange alongside new insights into the processes that shape the distribution of interior ocean carbon highlights the overall importance of variability at relatively smaller scales. Considering a range of processes that generate fluctuations at these scales, from basin-scale zonal asymmetries in the large-scale circulation to the eddies and filaments that dominate variability throughout the ACC to the intense extratropical cyclones that populate the Southern Hemisphere atmosphere year-round, this review seeks to call attention to important knowledge gaps that remain. Before discussing the four-dimensional variability, however, the dominant drivers governing the flow of carbon in the modern ocean and the main methods used to observe the carbon cycle in the Southern Ocean are briefly reviewed.

2. BACKGROUND

2.1. Processes Impacting the Oceanic Carbon Cycle

In general, the uptake, transport, and storage of carbon by the ocean result from the superposition of many different physical and biogeochemical processes that operate across a vast range of spatiotemporal scales, many of which can interact in complex ways. The air–sea flux of CO_2 (F_{CO_2}) is determined by the difference in the partial pressure of CO_2 (pCO_2) in the atmospheric and oceanic boundary layers, as well as numerous processes that control the transfer of gases between the two (Woolf et al. 2019). The rate of gas exchange, which ultimately occurs at the molecular level along the air–water interface, is strongly influenced by not only wind speed but also waves, surface currents, chemical enhancement, surfactants, and sea ice (M. Yang et al. 2021, Fairall et al. 2022). The pCO_2 in the marine atmospheric boundary layer (pCO_2^{air}) depends primarily on the mole fraction of CO_2 in dry air, with additional modulation due to variability in sea level pressure and saturation pressure of water vapor, which is determined by surface seawater temperature (T) and salinity (S). Similarly, oceanic pCO_2 (pCO_2^{sea}) depends on the concentration of dissolved inorganic carbon (DIC) but is also impacted by the acid-neutralizing capacity of seawater, which together with T, S, and pressure controls the distribution of DIC among its four aqueous phases [dissolved CO_2, carbonic acid (H_2CO_3), and bicarbonate (HCO_3^-) and carbonate (CO_3^{2-}) ions] (Dickson 2010).

The solubility of CO_2 in seawater has a well-known inverse relationship with T, such that warming (cooling) induces an increase (decrease) in oceanic pCO_2 (Takahashi et al. 1993). Using

this temperature dependence, variability in pCO_2 is often separated into thermal and nonthermal components, where the latter represents the change in pCO_2 due to variability in DIC and total alkalinity (a conservative measure of the ability of seawater to neutralize acids) (Takahashi et al. 2002). The distribution in the surface ocean of both inorganic carbon and alkalinity thus plays an important role in determining F_{CO_2} by governing the nonthermal variability in surface-ocean pCO_2.

The concentrations of DIC and alkalinity in the surface ocean, as well as the interior, are controlled by both physical and biogeochemical mechanisms (Sarmiento & Gruber 2006, Williams & Follows 2011). Like all dissolved tracers, DIC and alkalinity are subject to the full spectrum of physical processes acting in the ocean, which can broadly be separated into advection (lateral and vertical) and mixing (isopycnal and diapycnal). In addition, biological activity in the ocean plays a dominant role in setting the concentrations of DIC and alkalinity, through both the production and respiration of organic carbon and the precipitation and dissolution of particulate inorganic carbon, i.e., calcium carbonate. When these forms of biologically generated carbon are transported out of the sunlit upper ocean before remineralization, the net effect shifts inorganic carbon from the surface layer to deeper waters, in what is called the biological carbon pump. The export of organic carbon and calcium carbonate away from the surface ocean, which governs the efficiency of the biological pump, is achieved not only by gravitational sinking of particles but also by numerous mechanisms that induce vertical motions across a wide range of spatiotemporal scales (Siegel et al. 2023).

The oceanic carbon cycle in the contemporary ocean is extensively impacted by the accelerating addition of carbon to the atmosphere due to fossil fuel burning and land use changes (Gruber et al. 2023). To facilitate scientific understanding, the flow of carbon through the ocean is thus often separated, at least conceptually, into natural and anthropogenic components (Gruber et al. 2019a). While the latter traces C_{ANT} from its absorption at the air–sea interface through its subsequent transport and storage in the ocean interior, the natural carbon cycle describes the flow of carbon in the preindustrial ocean (DeVries 2014, Holzer & DeVries 2022).

2.2. Methods for Observing the Carbon Cycle in the Southern Ocean

Observations form the foundation of our knowledge of the Southern Ocean carbon cycle and its interactions with the global climate system. Modern shipboard measurements, which are the gold standard in terms of both accuracy and precision (Dickson 2010), make up the vast majority of in situ observations of the marine carbonate system in the Southern Ocean. Surface seawater pCO_2, along with T and S, is directly measured from underway research vessels and volunteer ships; quality-controlled data are collected and disseminated via the Surface Ocean CO_2 Atlas (SOCAT) (Bakker et al. 2016). Subsurface sampling of carbon parameters such as DIC and alkalinity is carried out primarily by oceanographic research vessels, which typically also measure biogeochemical variables like dissolved oxygen and macronutrients, in addition to T and S (Talley et al. 2016). Observations of carbon parameters in the open ocean are assembled, quality-controlled, and merged by the Global Ocean Data Analysis Project (GLODAP) (Olsen et al. 2016). Changes in C_{ANT}, which cannot be directly measured in seawater, are inferred from concurrently observed biogeochemical properties based on the differential impacts of anthropogenic and natural carbon cycling on those quantities (Clement & Gruber 2018). Because of the region's remote nature and extreme environmental conditions, shipboard datasets are sparse in the Southern Ocean, with strong biases spatially as well as seasonally (**Figure 2*a*,*b***).

Aside from shipboard measurements, a variety of other platforms and techniques have been used to observe aspects of the carbon cycle in the Southern Ocean. Remote sensing of ocean color and other optical properties provides insight into biologically driven impacts on carbon cycling

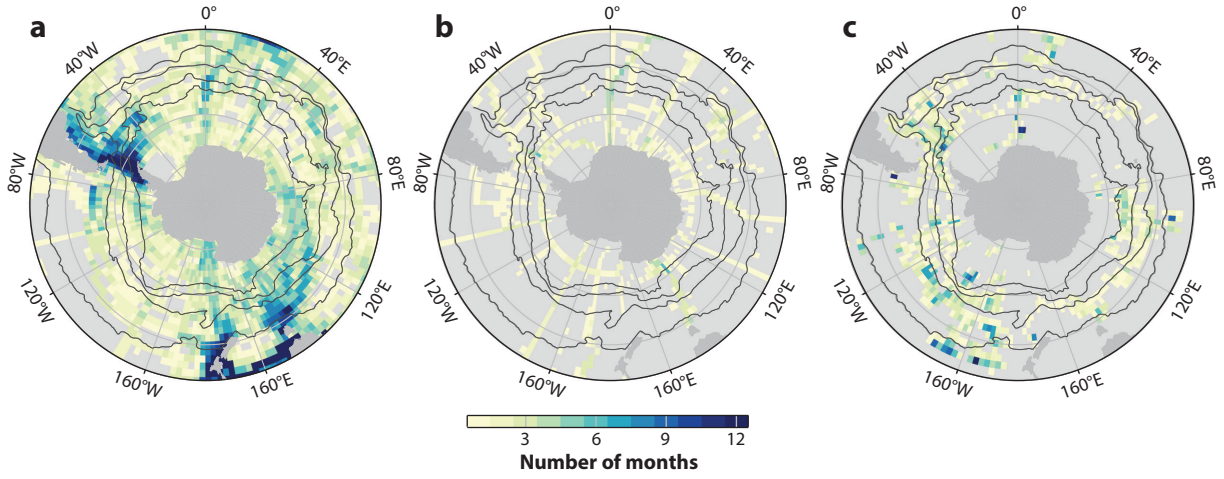

Figure 2

Number of unique months sampled in each 1° square for (*a*) pCO_2 measurements in the Surface Ocean CO_2 Atlas (SOCAT) dataset, 2001–2020; (*b*) dissolved inorganic carbon measurements in the Global Ocean Data Analysis Project (GLODAP) dataset, 2001–2020; and (*c*) pCO_2 estimates derived from pH measurements in the Southern Ocean Carbon and Climate Observations and Modeling (SOCCOM) dataset, 2014–2017. The thin black lines show, from north to south, the Subtropical Front (Gray et al. 2018) and the Sub-Antarctic Front, the Polar Front, and the Southern Antarctic Circumpolar Current Front (Kim & Orsi 2014).

in the surface ocean (Siegel et al. 2023), and satellite-based measurements of surface winds are critical for assessing gas transfer rates globally (Wanninkhof et al. 2009). Observations of carbon and oxygen in the atmosphere have been used to infer F_{CO_2} in the Southern Ocean (Resplandy et al. 2018, Nevison et al. 2020, Long et al. 2021). Temporal variability in the Southern Ocean carbon cycle has been directly assessed using mooring-based carbon measurements in coastal Antarctic waters (e.g., Arroyo et al. 2020, B. Yang et al. 2021) and in the Sub-Antarctic region just south of Australia (Shadwick et al. 2015), but the harsh conditions and vigorous flows associated with the ACC largely preclude moored observations in most of the open Southern Ocean.

The challenges inherent in shipboard operations within the Southern Ocean and the resulting limited data coverage make the use of autonomous instruments particularly attractive in this region (Bushinsky et al. 2019b). The earliest autonomous observations of surface-ocean pCO_2 were collected from drifting buoys (Boutin et al. 2008, Resplandy et al. 2014). More recently, uncrewed surface vehicles have been equipped with a suite of sensors that concurrently measure atmospheric and oceanic CO_2, together with barometric pressure and wind speed and direction (Sutton et al. 2021, Nicholson et al. 2022). Over the past two decades, the Argo array of autonomous profiling floats has exponentially increased coverage of subsurface *T* and *S* observations in the Southern Ocean (Johnson et al. 2022), and deployments of Biogeochemical Argo floats in this region have grown rapidly in the last 10 years, in large part due to the Southern Ocean Carbon and Climate Observations and Modeling (SOCCOM) program (Sarmiento et al. 2023). Although these floats are not capable of direct measurements of carbon at the present time, many of them do measure pH, which can be combined with empirical estimates of alkalinity (determined from simultaneous measurements of *T*, *S*, oxygen, and nitrate) to infer DIC and pCO_2 in the upper 2,000 m (Williams et al. 2017). Compared with direct measurements, oceanic carbon values derived in this way have larger uncertainty and are likely biased slightly high in the Southern Ocean (Bushinsky & Cerovečki 2023, Coggins et al. 2023). The exact cause of this discrepancy remains an open area of investigation, with impacts potentially arising from biases in float-based pH measurements,

errors in the thermodynamic equilibrium constants used to convert pH to pCO_2, and/or systematic uncertainties in estimated alkalinity (Williams et al. 2017). Despite this disadvantage, the greatly expanded spatiotemporal coverage supplied by float-based estimates in the Southern Ocean provides valuable in situ data from regions and seasons that are severely undersampled by shipboard observations (**Figure 2*c***).

The most direct observations of F_{CO_2} rely on the eddy covariance method, based on the correlation between the turbulent variations in vertical wind velocity and atmospheric CO_2 (Yang et al. 2022). Due to the difficulty of making the required high-frequency measurements with sufficient precision at sea, eddy covariance–based estimates of F_{CO_2} remain limited, especially in polar environments (Watts et al. 2022). Most often, F_{CO_2} is instead determined from a bulk formula,

$$F_{CO_2} = k_g \, \Delta pCO_2 \, (1 - f_{ice}), \qquad 1.$$

where k_g, the gas transfer velocity, depends on the solubility of CO_2 in seawater and on wind speed via a parameterized, nonlinear relationship; $\Delta pCO_2 = pCO_2^{sea} - pCO_2^{air}$; and f_{ice} is fractional sea ice cover. Because atmospheric motions efficiently mix CO_2 on timescales of a few days, especially in the Southern Hemisphere, atmospheric CO_2 concentrations in the Southern Ocean are well characterized by monthly measurements taken at a handful of land-based stations. Thus, the greatest challenges in accurately estimating F_{CO_2} at the regional or global scale arise from uncertainties in the parameterization of the gas transfer velocity as well as from uncertainties introduced by interpolating sparse shipboard pCO_2 observations in time and across large spatial areas (Woolf et al. 2019).

A variety of different interpolation methods have been employed to create gridded estimates from the relatively sparse direct measurements of oceanic carbonate parameters, both at the surface and in the interior; these methods include statistical regression techniques (Rödenbeck et al. 2014, 2022), neural network–based algorithms (Landschützer et al. 2016, Bittig et al. 2018, Keppler et al. 2020), and a growing number of additional machine learning methods, some of which also incorporate numerical model output (Gregor et al. 2019, Gregor & Gruber 2021, Gloege et al. 2022, Zemskova et al. 2022). For the most part, algorithms trained on shipboard observations are global by design, and thus the data are often separated into biophysically relevant regions prior to learning the relationships between environmental predictor variables and the carbon measurement of interest.

Finally, although not the focus of this review, numerical simulations are incredibly valuable tools that have considerably advanced our knowledge of the Southern Ocean carbon cycle and its connections to the global climate system. In addition to providing initial estimates (i.e., priors) for many machine learning algorithms, models can more easily probe the mechanisms that impact the flow of carbon through the ocean than observations alone, especially at timescales relevant to climate variability, and can distinguish variability due to natural processes from anthropogenically driven changes (McKinley et al. 2020, Holzer & DeVries 2022). Increasingly, ocean physical and biogeochemical models are combined with a multitude of observational datasets through either direct data assimilation (Verdy & Mazloff 2017, Carroll et al. 2020) or inverse methods (DeVries 2014, 2022) to produce observationally constrained, physically consistent estimates of the time-varying oceanic carbon cycle.

Equipped with this basic understanding of the primary mechanisms that drive the oceanic carbon cycle and how they are observed in the Southern Ocean, we can now examine the canonical zonal mean view of the Southern Ocean carbon cycle in detail, together with the processes that generate this two-dimensional distribution.

3. THE ZONAL MEAN CARBON CYCLE

The Southern Ocean carbon cycle has traditionally been understood through a zonal mean framework, an approach justified by the dominance of the eastward-flowing ACC that is assumed to rapidly homogenize tracers longitudinally. The zonal averages of surface and interior ocean carbon properties presented here are determined from three observation-based products (**Figure 3**). Subsurface concentrations of DIC and C_{ANT}, based on data from 1972–2013 that have been adjusted to the year 2002, are taken from the GLODAPv2.2016b gridded climatology (Key et al. 2015, Lauvset et al. 2016). Surface quantities, including F_{CO_2}, k_g, f_{ice}, and atmospheric and oceanic pCO_2, are obtained from the SOCAT-based product computed by Landschützer et al. (2021), averaged over the period 2001–2020. To assess the impact of adding year-round float-derived pCO_2 data to this neural network–based product, a second gridded estimate of F_{CO_2} is also considered here that incorporates SOCCOM float observations from 2014 to 2017 along with the usual (primarily shipboard) measurements (Bushinsky et al. 2019a, Landschützer et al. 2019a). This product is averaged for 2014–2017 to highlight the impact of the float observations; thus, to properly compare the two, the more recent SOCAT-only estimate is also restricted to the years 2014–2017 and to open ocean areas, to match the lack of estimates in coastal waters in the combined product. To account for the growing evidence that pCO_2 calculated from float-measured pH is biased slightly

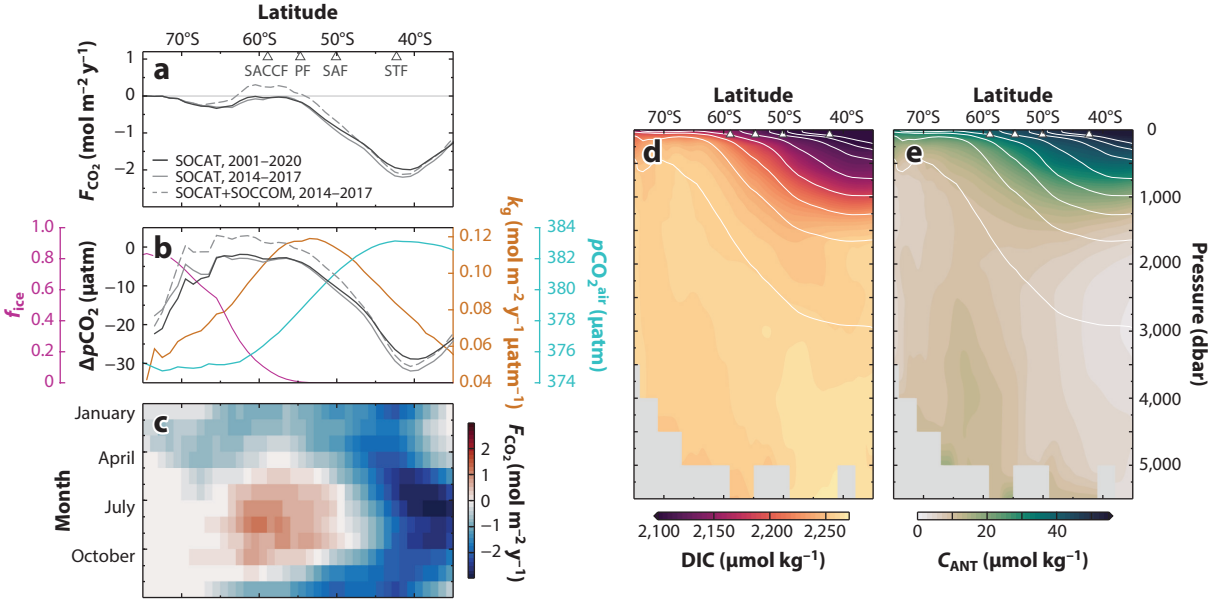

Figure 3

Zonal mean carbon properties in the Southern Ocean. (*a*) Annual mean air–sea CO_2 flux (F_{CO_2}) computed from gridded products based on the Surface Ocean CO_2 Atlas (SOCAT) and Southern Ocean Carbon and Climate Observations and Modeling (SOCCOM) datasets, with positive values indicating flux out of the ocean. (*b*) Annual mean 2001–2020 fractional sea ice cover (f_{ice}), gas transfer velocity (k_g), and atmospheric pCO_2 (pCO_2^{air}) from the SOCAT-based product along with annual mean $\Delta pCO_2 = pCO_2^{sea} - pCO_2^{air}$ from the products shown in panel *a*. (*c*) Monthly mean 2014–2017 F_{CO_2} computed from the SOCAT + SOCCOM–based product. (*d*,*e*) Dissolved inorganic carbon (DIC) concentration (panel *d*) and anthropogenic carbon (C_{ANT}) concentration (panel *e*) computed from the Global Ocean Data Analysis Project (GLODAP) climatology, referenced to the year 2002. White contours in panels *d* and *e* show the σ_θ surfaces for every 0.2 kg m^{-3} from 26.4 kg m^{-3} to 27.8 kg m^{-3}, computed from the GLODAP climatology; triangles in panels *a*, *d*, and *e* show the mean latitude of the Subtropical Front (STF) from Gray et al. (2018) and the mean latitudes of the Sub-Antarctic Front (SAF), Polar Front (PF), and Southern Antarctic Circumpolar Current Front (SACCF) from Kim & Orsi (2014).

high, the combined F_{CO_2} estimate shown here was constructed using float pCO_2 data that were first uniformly reduced by 4 μatm (Bushinsky et al. 2019a). This choice reflects the mean offset between float-based pCO_2 and nearby shipboard observations at the time the flux product was created; however, the precise value and cause of a systematic error in float-derived pCO_2 remain under active investigation.

Zonally averaged, the annual mean Southern Ocean F_{CO_2} exhibits a strong meridional gradient (**Figure 3*a***), which is linked to the spatial distribution of the circumpolar hydrographic fronts that separate the different water masses in the upper part of the Southern Ocean (Orsi et al. 1995, Kim & Orsi 2014) (**Figure 1*e***). The greatest uptake occurs in the northernmost portion of the domain, reaching 2 mol m^{-2} y^{-1} into the ocean immediately north of the mean latitude of the Subtropical Front (STF). Moving poleward from this peak, the magnitude of F_{CO_2} into the ocean decreases steadily until just south of the Polar Front (PF), which approximately aligns with the center of the ACC. In the region between the PF and the Southern ACC Front (SACCF), near-zero annual mean uptake is found in the estimates based solely on SOCAT pCO_2 observations. Combining these data with pCO_2 estimates from the SOCCOM dataset, however, produces significantly more outgassing at these latitudes, up to 0.3 mol m^{-2} y^{-1} out of the ocean in the annual mean. The gradient in zonal mean F_{CO_2} changes sign just south of the SACCF, associated with a poleward increase in carbon uptake that reaches a local peak of 0.3 mol m^{-2} y^{-1} into the ocean at approximately 66°S before tapering to zero due to the reduction in ice-free surface area approaching coastal Antarctica.

Integrating across the entire Southern Ocean south of 35°S gives an annual net oceanic carbon uptake of 1.1 ± 0.25 Pg y^{-1} for the period 2001–2020 based on the SOCAT data product. The given uncertainty estimate (±1 standard deviation) combines the error on the mean associated with interannual variability and a 0.15 Pg y^{-1} estimate of method uncertainty for the entire Southern Ocean, following Bushinsky et al. (2019a). Considering only the time period for which float-derived observations were incorporated (2014–2017) produces a slight increase in the annual net uptake based on SOCAT data alone, to 1.2 ± 0.15 Pg y^{-1}. Including SOCCOM data decreases the mean uptake for this shorter time period by 0.2 Pg y^{-1}, resulting in an annual mean F_{CO_2} of 1.0 ± 0.15 Pg y^{-1} into the ocean for the region south of 35°S. These two estimates are not statistically different given their significant uncertainties, which stem primarily from the sizable uncertainty introduced by the interpolation process. The relative difference between the two estimates approximately doubles when considering only the region south of 44°S, where the SOCAT-based product gives a 0.47 ± 0.11 Pg y^{-1} uptake that is reduced to 0.31 ± 0.11 Pg y^{-1} with the addition of SOCCOM data, but still falls short of statistical significance given the mapping uncertainty.

In the Southern Ocean, latitudinal variability in the annual and zonal mean F_{CO_2} is driven primarily by ΔpCO_2, the difference in pCO_2 between the ocean and the atmosphere, although the presence of sea ice significantly modulates F_{CO_2} in the more southern part of the domain (**Figure 3*b***). The gas transfer velocity, which is elevated throughout the mean latitude range of the ACC and peaks just north of the PF, does not control the variations in F_{CO_2} but does contribute to the overall strength of gas exchange within the ACC relative to other parts of the global ocean. The zonal mean distribution of ΔpCO_2 largely reflects surface-ocean pCO_2 variability but is also impacted by the almost 10-μatm drop in average atmospheric pCO_2 across the Southern Ocean, which occurs because of the poleward decrease in both sea surface temperature and sea level pressure.

The substantial seasonal variability in F_{CO_2} found throughout this region (**Figure 3*c***), which is largely concealed by the annual average, further emphasizes the dominant role of surface-ocean pCO_2 in regulating Southern Ocean carbon uptake. North of approximately 45°S, in the region of greatest annual net uptake, the ocean takes up carbon from the atmosphere year-round. The peak

in monthly averaged F_{CO_2} occurs equatorward of the average location of the STF during June and July, extending northward from the maximum in annual mean F_{CO_2}. The vigorous uptake in austral winter (June–September) at the northernmost edge of the Southern Ocean is offset by near-zero F_{CO_2} in the summer months at those latitudes. This phasing of the annual cycle indicates that surface heating in summer and cooling in winter drive the seasonal variability in surface-ocean pCO_2 via thermal effects on solubility.

In contrast, south of the Sub-Antarctic Front (SAF), spring and summer uptake transitions to outgassing from May to October. The strength of the maximum winter outgassing increases south of the PF, with the peak occurring in August just poleward of the mean latitude of the SACCF. South of 65°S, widespread (albeit weak) summer uptake becomes the dominant signal, as the presence of sea ice inhibits air–sea gas exchange during much of the rest of the year. The opposite phasing of the seasonal cycle here, as compared with the more northern part of the domain, indicates that nonthermal effects dominate changes in surface-ocean pCO_2 in the high-latitude portion of the Southern Ocean. The general diametric nature of the seasonal cycles in pCO_2 in subtropical and subpolar regions is well known (Takahashi et al. 1993). Recent observational analysis of year-round float observations in the Pacific sector expanded on this greatly, demonstrating that the shift from thermal to nonthermal control of the surface pCO_2 seasonal cycle is determined by the seasonal fluctuations in surface T, which are themselves set by meridional gradients in wintertime mixed-layer depth (Prend et al. 2022b).

The nonthermal processes that dominate the seasonal changes in surface-ocean carbon south of the STF result in pCO_2 dropping precipitously in spring, remaining low during summer, and then increasing throughout autumn before reaching a late-winter maximum. This seasonal cycle results primarily from the annual variation in photosynthesis, which converts inorganic carbon into organic material during spring and summer but becomes increasingly light limited during autumn and winter, especially at higher latitudes (Takahashi et al. 1993, Joy-Warren et al. 2019). Although primary production drives oceanic carbon uptake at all latitudes in the Southern Ocean, it does not fully deplete macronutrients in the surface layer, resulting in one of the world's largest high-nutrient, low-chlorophyll regions (Sarmiento & Gruber 2006, Arteaga et al. 2020) (**Figure 1*f***). Both light and iron limitation contribute to the inefficient utilization of nutrients in the Southern Ocean (Arteaga et al. 2019), with the former caused by the seasonal cycle of solar insolation and the latter attributed mostly to the lack of continental dust sources in the mid- and high-latitude Southern Hemisphere (Tagliabue et al. 2014).

Superimposed on the substantial biologically mediated seasonal variability in zonal mean F_{CO_2} are the changes due to the physical transport of carbon into and out of the mixed layer, driven by a range of upper-ocean processes that can vary seasonally in different ways. While the detailed physical mechanisms that generate tracer exchange across the base of the mixed layer remain an area of active research (Morrison et al. 2022, Taylor & Thompson 2023), the annual net effect in the Southern Ocean increases DIC in the surface ocean, thereby countering the impact of the biological carbon pump. Furthermore, while surface heat fluxes and biological production govern the seasonal cycle of zonal mean surface pCO_2 north and south of the STF, respectively, in the annual mean physical processes exert primary control on its meridional distribution. In the broadest sense, divergence in the wind-driven, meridional Ekman transport, caused by latitudinal gradients in the Southern Hemisphere westerly winds, leads to upwelling in the upper ocean south of the PF and downwelling north of the SAF (**Figures 1*c*** and **4**). This differential vertical motion acts on the negative vertical gradient in DIC in the upper ocean to produce a negative meridional gradient in surface DIC in the Southern Ocean (Wu et al. 2019). The negative vertical gradient in DIC is maintained by the biological pump, as is the case throughout the global ocean, but in the Southern Ocean it is further enhanced by the large-scale circulation.

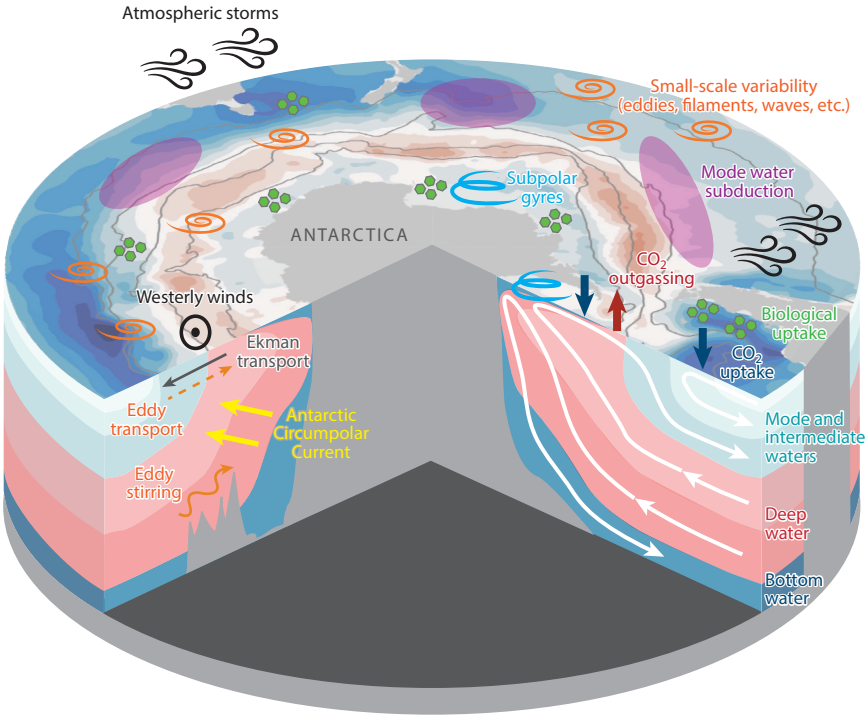

Figure 4

Schematic of the primary processes impacting the flow of carbon through the Southern Ocean. The vertical section on the right depicts the two-dimensional carbon cycle that results from zonally and temporally averaging the four-dimensional variability.

In addition to regulating surface-ocean pCO_2, the large-scale circulation in the Southern Ocean also governs the zonal mean interior distributions of DIC and C_{ANT} (**Figure 3*d*,*e***), which are predominantly aligned with contours of potential density (σ_θ). This circulation is intimately linked to the unique lack of continental barriers in the Southern Ocean, which prevents a geostrophic poleward boundary current from developing to balance the enormous amount of northward Ekman transport across the ACC. The circumpolar nature of the resulting large-scale flow thereby allows the vertical motions induced by the considerable surface divergence to extend far down into the deep ocean (Munk & Palmén 1951). The large-scale pattern in Ekman-driven upwelling and downwelling thus acts, in a zonally averaged sense, to pull dense waters up to the surface south of the PF and push them deeper north of the SAF. The resulting sharp incline of the isopycnals within the ACC (**Figure 3*d*,*e***) is associated with a meridional pressure gradient that supports the tremendous zonal flow of the geostrophically balanced ACC. Furthermore, the increase in potential energy generated by the wind-driven steepening of the isopycnals fuels the growth of baroclinic instabilities, resulting in the vigorous mesoscale eddy field that completely dominates the flow in the Southern Ocean at any instant in time (Nowlin & Klinck 1986). The net impact of these time-varying fluctuations converts some of the added potential energy to eddy kinetic energy, which, in the time and zonal mean, creates an overturning circulation that flattens the isopycnals, opposing the circulation forced by the large-scale winds. The sum of the wind- and eddy-driven circulations, both of which are large but nearly compensating, gives the residual overturning circulation, which describes the effective mass transport in the time and zonal mean (Marshall & Speer 2012).

The residual flow in the Southern Ocean largely aligns with the zonal mean isopycnals, driving adiabatic upwelling of the dense ($\sigma_\theta \geq 27.6$ kg m^{-3}) waters that flow southward into the Southern Ocean from the Atlantic, Indian, and Pacific Oceans at depths greater than 1,500 m (**Figure 4**). The return of these deep water masses to the surface layer, which occurs predominantly south of the PF in the high-latitude Southern Ocean, represents a key link in the global meridional overturning circulation (Talley 2013). In general, deep waters are naturally enriched in inorganic carbon due to the remineralization of organic matter that rains down from the productive surface ocean during the decades to centuries that these waters spend transiting the basins to the north while at depth (Williams & Follows 2011). At the same time, the isolation of these waters from the atmosphere for so long means they have negligible concentrations of C_{ANT} (Gruber et al. 2019a). Thus, by transporting this water into the upper reaches of the Southern Ocean, the meridional overturning circulation generates the large-scale zonal mean patterns observed in the interior, with maximum DIC and minimum C_{ANT} concentrations found in the deep water masses that enter the Southern Ocean from the north (**Figure 3*d*,*e***).

Once at the surface, the strong Ekman transport advects this water either northward toward the SAF, where it subducts and becomes Antarctic Intermediate Water, or southward into the subpolar and coastal regions, where it sinks and becomes Antarctic Bottom Water (**Figure 4**). The latter process is driven by buoyancy losses at the surface, occurring largely in coastal polynyas in winter, caused by substantial heat fluxes as well as the addition of salt due to brine rejection during sea ice formation (Ohshima et al. 2016). Freshwater fluxes are also central to the former process, as the sea ice that was formed at higher latitudes is advected equatorward by Ekman dynamics and melts at more northern latitudes (Abernathey et al. 2016, Haumann et al. 2016). In both cases, the increases in $F_{\mathrm{CO_2}}$ into the ocean as these waters move meridionally in the Ekman layer are typically attributed to a combination of biological production of organic carbon (supported by the elevated macronutrients found in upwelled deep water) and high potential for anthropogenic uptake (due to the long time since these waters were last in contact with the atmosphere) (Gruber et al. 2019b). The increased C_{ANT} concentration in Antarctic Bottom Water and Antarctic Intermediate Water is thus seen as reflecting the ventilation of the deep waters of the globe in the Southern Ocean surface layer before incorporation into these newly formed water masses (**Figure 3*e***). In the zonal mean sense, both Antarctic Bottom Water and Antarctic Intermediate Water are exported equatorward, where they play critical roles in the global cycling of heat, freshwater, and nutrients in addition to carbon.

The lighter Sub-Antarctic Mode Water (SAMW) ($\sigma_\theta \leq 27.0$ kg m^{-3}), which extends as deep as 500 m in the northern portion of the Southern Ocean, is also advected equatorward after it forms near the SAF. Like all mode waters, SAMW is created in a seasonal process involving the generation of extremely deep mixed layers during winter followed by springtime restratification that isolates the remnant well-mixed layer from the atmosphere. In the zonal average, the lowest subsurface DIC values in the region are found in the SAMW, but it also contains some of the highest concentrations of C_{ANT} in the global ocean (**Figure 3*d*,*e***). These characteristics predominantly reflect CO_2 exchange in the subtropical waters that are advected southward in the surface ocean from more northerly latitudes, according to both modeling and inverse-based studies (DeVries 2014, Iudicone et al. 2016, Davila et al. 2022). Only recently, however, have autonomous observations enabled questions regarding carbon cycling in SAMW to be addressed using widespread, year-round, in situ measurements. In particular, the change in water mass properties required to transform warm, salty subtropical waters into cool, fresh SAMW (which simultaneously promotes uptake of atmospheric CO_2 through solubility effects) occurs upstream of the formation sites of SAMW (Fernández Castro et al. 2022). Moreover, active uptake of atmospheric carbon by the ocean was not observed in the regions of maximum mixed-layer depth during winter, suggesting

that air–sea carbon flux and mode water formation are decoupled in space and time (Bushinsky & Cerovečki 2023).

Although advection associated with the large-scale circulation is the usual mechanism invoked to describe the carbon cycle of the Southern Ocean, mixing likely plays an equally important role in this region (Gille et al. 2022, Morrison et al. 2022). Both isopycnal and diapycnal mixing have been estimated to be significant in the Southern Ocean, facilitated by the intense mesoscale eddy field and strong tracer gradients (Watson et al. 2013, Garabato et al. 2017). The full impact of mixing processes on carbon cycling in the Southern Ocean remains poorly constrained from observations.

Overall, the two-dimensional, zonally averaged picture presented in this section (**Figure 4**) has enabled significant advances in our understanding of the Southern Ocean carbon cycle, especially on timescales of decades and longer. As observational and modeling capabilities have dramatically expanded over the recent decade, however, the importance of deviations from the zonal mean has become increasingly apparent. Starting with the basin scale and then moving to the mesoscale and smaller, the following two sections discuss what is currently known regarding variability in the Southern Ocean carbon cycle and what challenges remain for understanding the governing processes and the interactions between these scales and global climate variability.

4. LARGE-SCALE ZONAL ASYMMETRY

A growing body of research has demonstrated the importance of zonal asymmetry in many Southern Ocean phenomena, including mixed-layer depth (Sallée et al. 2010), winds (Fogt et al. 2012), upper-ocean heat (Tamsitt et al. 2016), phytoplankton (Noh et al. 2021), and sea ice (Schroeter et al. 2023). Indeed, the ACC does not follow a purely zonal path; rather, it gradually shifts poleward by almost 20° from its northernmost location just downstream of the Drake Passage until it reaches its southernmost extent in the Ross Sea region (**Figure 1*b***). Averaging along a latitude circle thus convolves numerous different dynamical and biogeochemical regimes, which can obfuscate process-level understanding. Even if the Southern Ocean is considered in an along-stream coordinate system aligned with the mean flow of the ACC, the various physical processes that generate the meridional overturning circulation are not required to be uniformly distributed or coincident in space and time. To the contrary, the zonally asymmetric distribution of topography in the Southern Ocean (**Figure 1*a***) fundamentally impacts the circulation of the ACC, which was shown analytically by Marshall (1995) and subsequently demonstrated using surface observations (Sallée et al. 2011, Thompson & Sallée 2012). More recently, interaction between the ACC and the topographic features that intersect its path has been identified as a critical factor governing the upwelling of northern-sourced deep waters within the ACC in high-resolution models (Tamsitt et al. 2017, Cai et al. 2022, Yung et al. 2022).

Investigation into large-scale zonal asymmetry in the Southern Ocean carbon cycle initially focused on the uptake and storage of C_{ANT} in Southern Ocean mode waters. Sallée et al. (2012) used climatological estimates of subduction and C_{ANT} to show that the transfer of C_{ANT} across the base of the mixed layer occurs at specific locations within the Southern Ocean, which are associated with mode waters with distinct σ_θ values. This localization results from variability in the mechanisms that drive subduction (Ekman transport, eddy advection, and changes in mixed-layer depth) and how these interact with the variability in C_{ANT}. More recent estimates of C_{ANT} reveal similar basin-scale differences within the SAMW density range, with the highest concentrations in the Indian sector mode waters and the lowest in the Pacific (**Figure 5*j–l***). Given the importance of SAMW in global C_{ANT} sequestration, the recognition of these zonal asymmetries motivated significant interest in the spatiotemporal variability of mode water formation,

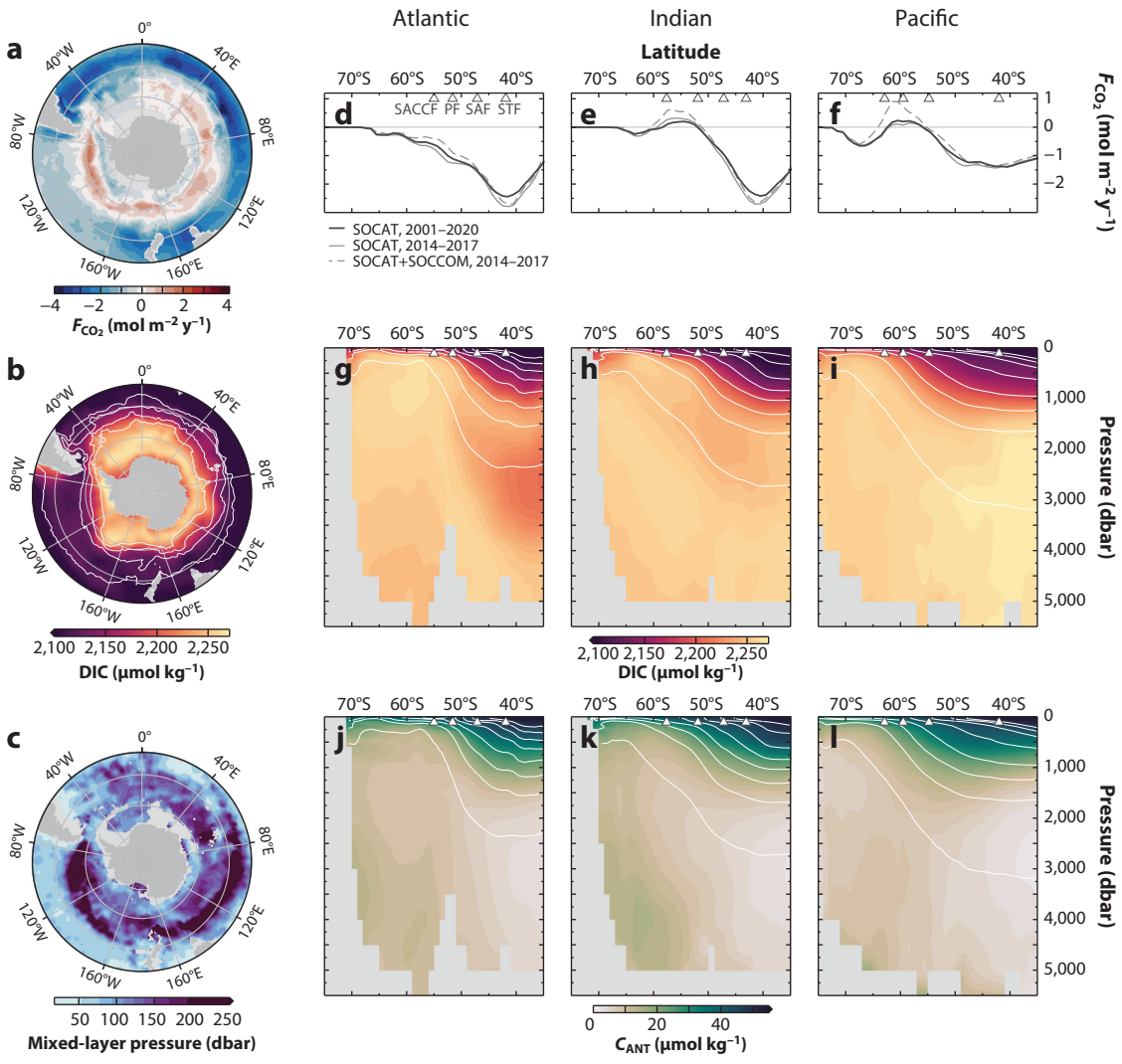

Figure 5

Zonally asymmetric carbon properties in the Southern Ocean. (*a*) Annual mean 2014–2017 air–sea CO_2 flux (F_{CO_2}) computed from the gridded product based on the Surface Ocean CO_2 Atlas (SOCAT) and Southern Ocean Carbon and Climate Observations and Modeling (SOCCOM) datasets, with positive values indicating flux out of the ocean. (*b*) Dissolved inorganic carbon (DIC) at 200 m from the Global Ocean Data Analysis Project (GLODAP) climatology, referenced to the year 2002. (*c*) Median pressure at the base of the mixed layer in September from the Global Ocean Surface Mixed Layer Statistical Monthly Climatology (Johnson & Lyman 2022). (*d–l*) Longitudinal averages within the Atlantic sector (70°W–25°E), the Indian sector (25°E–150°E), and the Pacific sector (150°E–70°W) of annual mean F_{CO_2} computed from gridded products based on the SOCAT and SOCCOM datasets (panels *d–f*) and DIC (panels *g–i*) and anthropogenic carbon (C_{ANT}) (panels *j–l*) computed from the GLODAP gridded climatology, referenced to the year 2002. White contours in panels *g–l* show the σ_θ surfaces for every 0.2 kg m^{-3} from 26.4 kg m^{-3} to 27.8 kg m^{-3}, computed in each sector from the GLODAP climatology; triangles in panels *d–l* show the mean latitude of the Subtropical Front (STF) from Gray et al. (2018) and the mean latitudes of the Sub-Antarctic Front (SAF), Polar Front (PF), and Southern Antarctic Circumpolar Current Front (SACCF) from Kim & Orsi (2014) for each sector.

subduction, and transport (Morrison et al. 2022). However, the interactions between the processes that create mode waters and the factors that govern the carbon content of those waters (both C_{ANT} and DIC) are less well characterized from observations. Using year-round circumpolar observations collected by Biogeochemical Argo floats, Bushinsky & Cerovečki (2023) recently found negligible zonal variability in the distribution of biogeochemical properties on isopycnal surfaces across the different SAMW formation regions. The observed basin-scale differences in mode water carbon concentrations can therefore be attributed to systematic variations in the potential density of SAMW formed in different sectors of the Southern Ocean.

Zonal asymmetry also plays a significant role in both the mean and variability of Southern Ocean F_{CO_2} according to flux estimates computed from SOCAT pCO_2 observations. Differences in decadal variability among the Atlantic, Indian, and Pacific sectors have been identified and attributed to zonally asymmetric changes in the large-scale wind field (Keppler & Landschützer 2019, Landschützer et al. 2019b). Within the ACC, considerable basin-scale differences in annual mean F_{CO_2} have also been recently highlighted using float-based flux estimates averaged within frontal regions instead of by latitude (Prend et al. 2022a). While the Indo-Pacific sector of the ACC is dominated by outgassing of CO_2 to the atmosphere, the Atlantic sector takes up a considerable amount of carbon (**Figure 5*a***). Furthermore, this divergence results from differences in the annual mean surface-ocean pCO_2, as opposed to differences in its seasonal cycle or in the parameterized gas transfer velocity. Although the addition of float-based pCO_2 data accentuates this spatial variability, the differences between F_{CO_2} in the Atlantic and in the Indo-Pacific are apparent even in basin-scale zonal averages of fluxes computed from SOCAT measurements alone (**Figure 5*d–f***).

Several factors can potentially explain the observed regional variability in the mean surface-ocean pCO_2, including variations in the biological carbon pump, solubility effects, and physical processes. By analyzing subsurface observations from Biogeochemical Argo floats, Prend et al. (2022a) demonstrated that the observed basin-scale deviations in surface-ocean pCO_2 can be completely accounted for by differences in the transfer of high-carbon waters from the interior ocean into the mixed layer at the end of winter, a process known as obduction. Crucially, the resulting variation in surface-ocean pCO_2 is driven primarily by the basin-scale differences in the maximum depth of the winter mixed layer and less so by variations in the carbon distribution of the obducted waters. Indeed, the carbon properties of the waters just below the mixed layer (at depths near 200 m) are fairly homogeneous across all portions of the ACC, but the distribution of wintertime mixed-layer depths clearly separates the Atlantic from the Indian and Pacific sectors (**Figure 5*b*,*c***). The large regional variability in the maximum mixed-layer depth, coupled with the strong vertical gradient in carbon within the ACC, results in significant differences in surface-ocean pCO_2 and thus F_{CO_2}. This observation-based finding is supported by numerical studies examining Lagrangian pathways into the mixed layer from the interior Southern Ocean (Viglione & Thompson 2016, Tamsitt et al. 2017).

While the transfer of waters across the base of the mixed layer appears to be a key mechanism governing the spatial variability in F_{CO_2}, the impact of this exchange on the carbon cycle also depends critically on the carbon properties of the waters in the interior ocean, and thus on the processes that set this distribution. Within the upper ACC, zonal variability in carbon properties below the mixed layer appears fairly minimal (**Figure 5*b***), likely due to mixing and stirring by the vigorous mesoscale and submesoscale motions found there (Brand et al. 2023). Much larger differences in subsurface carbon distributions are found to the north, however, closer to the source regions of the deep waters that flow into the Southern Ocean at its equatorward boundary (**Figure 5*g–l***). Differences in the inorganic carbonate properties of deep waters formed in the North Atlantic compared with those of Indo-Pacific origin can be explained by the separate

global pathways of these water masses before they enter the Southern Ocean, together with the vertical separation in the depths of remineralization of organic matter and particulate inorganic carbon (Chen et al. 2022).

Moving poleward into the subpolar portion of the Southern Ocean, the zonal asymmetry in the large-scale circulation becomes more evident due to the presence of separate cyclonic gyre circulations in the Ross and Weddell Seas (**Figure 1*b***). Careful analysis of shipboard transects from the Weddell region of the South Atlantic recently revealed the central importance of this horizontal circulation in driving the carbon cycle there (MacGilchrist et al. 2019). Deep waters upwelled to mid-depths in the open Southern Ocean circulate horizontally in the Weddell gyre, during which time the biological pump shifts DIC from the surface layer to intermediate depths. The correlation between DIC anomalies and the horizontal transport across the scale of the gyre has a first-order impact on the carbon cycle of this region, illustrating the importance of considering variability across sub-basin scales.

5. SMALL-SCALE VARIABILITY

As one of the most turbulent places on the planet, the Southern Ocean is replete with variability at all spatial and temporal scales. As Deacon (1937) first inferred based on observed salinity distributions, motions at the oceanic mesoscale [$\mathcal{O}$(100 km, 10 days)] have a leading-order impact on the circulation (Marshall & Speer 2012, Morrison et al. 2014) and mixing (Gille et al. 2022, Morrison et al. 2022) of the Southern Ocean. Submesoscale variability, characterized by scales of $\mathcal{O}$(1–10 km, 1 day), is also thought to have significant influence on ocean mixing and ventilation globally (Su et al. 2018) and in the Southern Ocean in particular (Zhang et al. 2023). In recent years, the influence of variability at the mesoscale on biogeochemical activity in the Southern Ocean has been investigated intensely as well, from organic carbon export (Llort et al. 2018) and cycling of nutrients (Patel et al. 2020) and iron (Ellwood et al. 2020) to impacts on phytoplankton (Dawson et al. 2018, Della Penna et al. 2018) and higher trophic levels (Della Penna et al. 2022). Carbon cycling in the Southern Ocean may be affected by variability at the mesoscale and smaller scales via these physical and biological pathways, as well as through high-frequency processes at the air–sea interface that directly impact gas exchange. Progress toward characterizing the full effects of small-scale variability on the Southern Ocean carbon cycle has been achieved using observational and numerical approaches in recent years, but many important questions remain outstanding.

Despite their ubiquity, a comprehensive accounting of the impacts of mesoscale variability on carbon uptake in the Southern Ocean, both direct and indirect, is still lacking. Cumulatively, these motions play a first-order role in the Southern Ocean meridional overturning circulation and the concomitant upwelling of DIC and C_{ANT} (Section 3). Additionally, mesoscale eddies may indirectly shape the carbon cycle via net changes in upper-ocean stratification and mixed-layer depth. Numerical simulations have provided evidence for global-scale impacts on ocean carbon through a number of mechanisms, including changes to alkalinity cycling, shifts in biological production, and effects on the export of organic carbon from the surface (Lévy et al. 2014, Munday et al. 2014, Dufour et al. 2015, Harrison et al. 2018, Krumhardt et al. 2020, Jersild et al. 2021). Such large-scale impacts on Southern Ocean carbon cycling are challenging to quantify directly due to the wide range of spatiotemporal scales and the variety of processes involved. Observational investigations of the role of mesoscale eddies, in contrast, often sample a single coherent vortex or consider only one process that influences carbon cycling in isolation, and in the Southern Ocean direct measurements of carbon parameters within mesoscale eddies are particularly rare.

In addition to these indirect influences, mesoscale eddies can also impact oceanic carbon uptake in a more direct manner, by inducing anomalies at the surface that locally modulate $F_{\mathrm{CO_2}}$;

these small-scale fluctuations can potentially affect the larger-scale Southern Ocean carbon cycle through rectification. Recent surveys in the Sub-Antarctic zone south of Australia found anomalously low surface-ocean pCO_2 and enhanced uptake inside an anticyclonic eddy (Jones et al. 2017) and anomalously high surface-ocean pCO_2 inside a cyclonic eddy (Moreau et al. 2017). Examining year-round observational records from the Drake Passage, Song et al. (2016) found significant correlation between mesoscale variability and surface-ocean pCO_2 that had a clear seasonal dependence. Using a high-resolution regional numerical simulation, they attributed the observed seasonal relationship to shifts in the balance between thermal and nonthermal controls, with subsurface vertical mixing identified as the key governing process in all seasons. Coupling with the atmosphere also led to significant changes in upper-ocean mixing in model studies, with likely ramifications for carbon exchange (Byrne et al. 2016, Song et al. 2020). Recent comprehensive measurements of the air–sea transition zone in an anticyclonic eddy in the Brazil–Malvinas Confluence region of the western South Atlantic demonstrated that both the ocean and atmosphere undergo adjustments that directly affect CO_2 gas exchange (Pezzi et al. 2021).

The full impacts of submesoscale motions on the physical drivers of the carbon cycle of the Southern Ocean remain poorly characterized. Although model-based studies have consistently indicated that submesoscales play a critical role in the physics of this region (Bachman et al. 2017, Balwada et al. 2018, Taylor et al. 2018), observational evidence has been exceedingly sparse, especially in the dynamic region of the ACC and the high-latitude regions covered in sea ice. Recently, measurements collected with autonomous gliders have begun to shed light on these important areas (Dove et al. 2021, 2023; du Plessis et al. 2022), indicating that mixing and stirring by the mesoscale and submesoscale have a significant role in ventilation and mixed-layer restratification. In addition, these impacts appear to extend deep into the water column, well beyond the surface mixed layer (Balwada et al. 2023). Submesoscale influences on biogeochemical processes have generally been tied to nutrient delivery into, and carbon export out of, the sunlit surface layer. In the high-nitrate Southern Ocean, iron is the limiting nutrient, and evidence from numerical simulations suggests that iron supply to the surface in this region is enhanced by submesoscale vertical motions (Uchida et al. 2019, 2020). Indeed, the vertical mixing of iron is a key factor determining variability in the biological pump in the Southern Ocean (Tagliabue et al. 2014, Stukel & Ducklow 2017).

Processes at even smaller spatiotemporal scales are known to have a significant impact on the ocean boundary layer yet are not explicitly accounted for in the gas transfer parameterizations used in large-scale flux estimates. Because of the strong westerly wind forcing, which generates extreme wave conditions along with the intense currents and mesoscale variability that characterize the Southern Ocean, these processes may be particularly significant in this region (Young et al. 2020). For instance, near-inertial waves have been found to significantly change F_{CO_2} in a high-resolution regional model (Song et al. 2019). Numerical simulations also suggest that Langmuir circulation can substantially modulate F_{CO_2} globally (Smith et al. 2018) and in the Southern Ocean specifically (Tak et al. 2023). Breaking waves, which introduce bubbles into the upper ocean and sea spray into the lower atmosphere, likely influence F_{CO_2} in the Southern Ocean in significant ways that are not fully appreciated (Deike 2022). In addition, the role of Antarctic sea ice is poorly understood, in terms of both its impacts on upper-ocean carbonate chemistry and biology and its direct influence on gas exchange, representing a dominant source of uncertainty in estimating carbon uptake in the ice-covered regions (Swart et al. 2019, Watts et al. 2022).

As the main source of the energy that drives motions in the Southern Ocean, mean surface winds in this region are known for their strength, but in reality, the Southern Ocean is filled with extratropical cyclones, i.e., storms (Priestley et al. 2020). Synoptic storms play a central role in the generation of ocean turbulence, thereby modulating the physical transport of carbon in the upper

water column as well as biological production and export, and also directly affect the rate of gas exchange. The impacts of Southern Hemisphere storms on the carbon cycle of the Southern Ocean have been difficult to observe with traditional methods. However, recent autonomous measurements in the region south of Africa revealed significant high-frequency variability in surface-ocean pCO_2 due to storm-driven mixing in the upper ocean (Nicholson et al. 2019, 2022). Variability at timescales associated with atmospheric storms also dominates the horizontal and vertical variability in phytoplankton observed in the Southern Ocean (Carranza et al. 2018, Prend et al. 2022c).

The large-scale impacts of small-scale variability on the carbon cycle of the Southern Ocean have been challenging to characterize, primarily because the wide range of spatiotemporal scales involved are not well captured by the historical observational record. Advancements in observing technologies, especially in autonomous sensing, are now enabling resolution of a much wider range of phenomena than ever before, which will open up new opportunities to investigate this question directly. At the moment, however, limited insights can be inferred by examining what is known about the influence of small-scale oceanic motions on the large-scale evolution of physical ocean properties. Detailed analysis of the mesoscale eddy field from satellite and float observations (Hausmann et al. 2017) provides compelling evidence that the spatiotemporal distribution of anticyclones and cyclones is not random. As a result, the changes that eddies induce in the upper ocean are not symmetric, leading to significant variability in the cumulative effect on mixed-layer depth across the Southern Ocean (**Figure 6*a*,*b***). Furthermore, spatial variability in Southern Ocean ventilation has been linked to localized regions of enhanced mesoscale eddy activity that occur downstream of the standing meanders generated where the ACC interacts with prominent topographic features (Dove et al. 2022). Temporal changes in eddy-driven mixing in the surface of the Southern Ocean have been linked to climate variability in the Southern Hemisphere (Busecke & Abernathey 2019), suggesting the possibility of a nonlinear carbon–climate feedback mechanism mediated through small-scale processes in the Southern Ocean. And while the Southern Ocean is stormy at all times of year, the Southern Hemisphere storm track is zonally asymmetric (Inatsu & Hoskins 2004, Hoskins & Hodges 2005), and the spatial patterns of storm activity change substantially over the seasonal cycle (Priestley et al. 2020) (**Figure 6*c*,*d***). Research is needed to better assess how these sources of variability shape the four-dimensional evolution of the Southern Ocean carbon cycle.

6. DISCUSSION

Considering this rapidly growing body of evidence, the picture of the Southern Ocean carbon cycle that emerges is fundamentally three-dimensional in space, with important variability at seasonal to subseasonal timescales, in contrast to the traditional focus on the zonal mean decadal variability. Biogeochemical differences in the deep waters that enter the basin, localization of upwelling and ventilation to specific places within the ACC, and lateral flow within the gyres of the subpolar Southern Ocean all shape the distribution of carbon in the interior. The exchange of carbon between the interior and the surface ocean directly exposed to the atmosphere is controlled primarily by the myriad of processes that govern mixed-layer depth variability and upper-ocean mixing, which are also non-uniformly distributed in space and time. Surface-ocean pCO_2 and F_{CO_2} are regulated therefore by surface forcing from winds as well as heat and freshwater fluxes, by small-scale variability that drives exchange across the base of the mixed layer, and by the large-scale circulation that sets up the interior carbon distribution. While challenging from both the observational and modeling perspectives because of the requirement to resolve a broad range of scales, improved understanding and representation of these processes and their interactions are needed to

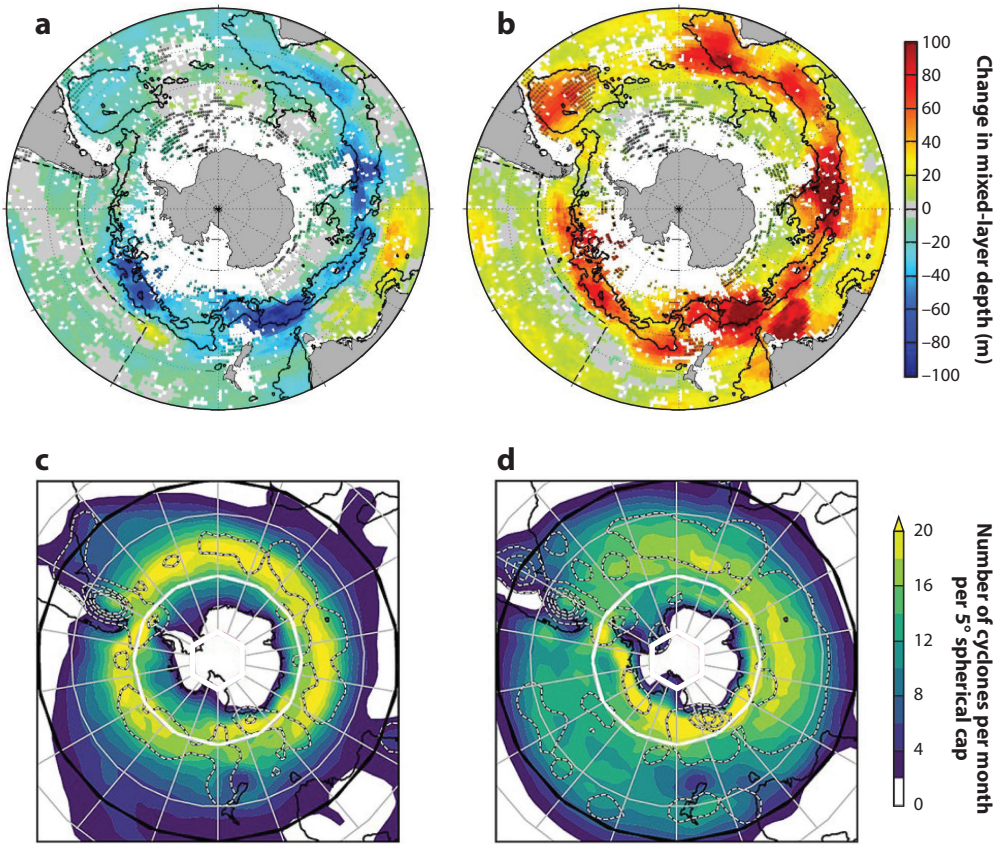

Figure 6

Asymmetric distributions of mesoscale eddy impacts and storms in the Southern Ocean. (*a*,*b*) Mean observed change in late-winter (August–October) mixed-layer depth due to cyclonic eddies (panel *a*) and anticyclonic eddies (panel *b*). Solid black contours outline regions of high eddy activity as determined from sea surface height variance. (*c*,*d*) Mean storm tracks (*colors*) and genesis locations (*dashed contours*) in summer (panel *c*) and winter (panel *d*) from European Centre for Medium-Range Weather Forecasts Reanalysis 5. Genesis density contours are given, in increments of 1, from 1 to 4 cyclones per month per 5° spherical cap. Panels *a* and *b* adapted with permission from Hausmann et al. (2017); copyright 2016 American Geophysical Union. Panels *c* and *d* adapted from Priestley et al. (2020) (CC BY 4.0).

significantly reduce uncertainties and advance our ability to predict the future evolution of this critical component of the global climate system.

This four-dimensional variability has strong implications for observing and modeling the Southern Ocean carbon cycle. Many of the important processes and phenomena in this region are unique, or at least near the end of the range of global oceanographic conditions. Furthermore, measurements at a single location are not likely to be representative of the entire circumpolar region; in the Southern Ocean in particular, advection dominates the variability observed at any one location (Nicholson et al. 2022). Similarly, observations across the full seasonal cycle and across the entire range of forcing conditions are needed to adequately capture the annual mean signal. Shipboard observations are inherently biased toward spring and summer and away from the extreme storms that populate the high-latitude Southern Ocean in all seasons. Indeed, underway shipboard pCO_2 measurement systems become contaminated by noise when wind speeds are greater than approximately 15 m s^{-1} (R. Wanninkhof, personal communication), conditions that

are met frequently in the Southern Ocean year-round (Young et al. 2020). The issues introduced by interpolating spatiotemporally biased data over large areas were clearly illustrated by Gloege et al. (2021), who provided irrefutable evidence that the distribution of carbon in the surface Southern Ocean is not well captured by the sampling coverage of direct pCO_2 observations.

The observation-based understanding reviewed here also has implications for modeling the Southern Ocean carbon cycle. In particular, because of the strong lateral and vertical gradients in carbon, variability in the small-scale processes that impact upper-ocean mixing appears to be centrally important in the Southern Ocean. Better representation of the variability in mixed-layer depth at seasonal and subseasonal timescales will likely produce substantial improvements in the ability of Earth system models to accurately simulate the carbon cycle of the Southern Ocean. Improving model capabilities to simulate the net effects of small-scale processes on isopycnal mixing and air–sea gas exchange should also be prioritized.

In general, a large disconnect still exists between the model-based understanding of (sub)mesoscale impacts on the Southern Ocean carbon cycle and observation-based studies that focus on a limited set of mechanisms and often target a single coherent vortex. Reconciling these at times heterogeneous views would be incredibly valuable for the community. Significant progress is needed to assess from observations the cumulative effects of small-scale variability on large-scale carbon cycling in the Southern Ocean and how such impacts may be rectified to shape observed patterns of zonal asymmetry and seasonal variability, as well as variability at longer timescales. Advancing process-level understanding at these scales is absolutely key to confidently predicting the future evolution of the Southern Ocean carbon cycle.

Although many outstanding questions remain, the pace of scientific discovery regarding carbon cycling in the Southern Ocean has never been faster than it is today. The substantial advances in the past decade have been enabled by significant investments in ocean observing in this region from the international community, together with improvements in model-based representation of the Southern Ocean. A sustained, widespread, year-round observing system for surface and subsurface biogeochemical properties in the Southern Ocean is a critical priority, as this provides the spatiotemporal data coverage required to understand large-scale variability. However, such sustained observing must also be supplemented with targeted studies that use autonomous and ship-based measurements to characterize the impact of small-scale and localized processes on carbon cycling throughout the full seasonal cycle and across the entire range of biogeochemical and physical conditions found in this dynamic region. This type of comprehensive observational approach to quantifying the mechanisms that control the large-scale uptake, storage, and transport of carbon in the Southern Ocean, although challenging to achieve, will undoubtedly catalyze significant scientific advances that have been heretofore unreachable, allowing numerical simulations to be evaluated and improved based on a mechanistic understanding. Improving observation-based understanding of the full four-dimensional variability in the carbon cycle of the contemporary Southern Ocean is urgent given the rapidly changing conditions in this critical polar environment and its central role in the global climate system.

SUMMARY POINTS

1. The connection between the surface of the Southern Ocean and the deep waters of the global ocean, driven by the large-scale overturning circulation, makes this remote region fundamentally unique and critically important within the carbon cycle of the entire planet.

2. Substantial zonal asymmetry exists in the distribution of carbon within the Southern Ocean, in both the mean and the variability, underscoring the need to move beyond the canonical zonal mean framework for understanding the carbon cycle in this region.
3. The cumulative impacts of oceanic turbulence, from the mesoscale to the microscale, on carbon cycling in the Southern Ocean are complex and poorly characterized. The effects of such motions on mixed-layer variability emerge as one crucial point of control.
4. Small-scale processes in the air–sea transition zone, especially those related to high-frequency atmospheric variability in the intense Southern Hemisphere storm tracks, likely have significant effects on carbon cycling in the Southern Ocean due to influences on both ocean mixing and gas exchange.
5. Advances in understanding and predicting the carbon cycle of the Southern Ocean will require a combination of sustained widespread biogeochemical measurements and novel approaches to expanding process-level measurements in crucial yet undersampled locations.

DISCLOSURE STATEMENT

The author has received research funding as part of the SOCCOM program.

ACKNOWLEDGMENTS

This work is dedicated to Stephen Riser, whose quiet leadership has transformed physical and biogeochemical observations in the Southern Ocean, and to Jorge Sarmiento, whose vision of the importance of the Southern Ocean in the global carbon cycle has provided unequaled inspiration to generations of oceanographers. Support was generously provided by the National Science Foundation through awards OPP-193622 and OCE-1756882, the National Oceanic and Atmospheric Administration through award NA20OAR4320271, and the Department of Energy through award DE-SC0022243. Channing Prend and an anonymous reviewer provided helpful feedback. The author gratefully acknowledges the dedicated efforts of countless people and agencies around the world who observe the ocean and make those measurements available to the global scientific community, especially those contributing to SOCAT, GLODAP, SOCCOM, and the International Argo Program.

LITERATURE CITED

Abell JT, Winckler G, Anderson RF, Herbert TD. 2021. Poleward and weakened westerlies during Pliocene warmth. *Nature* 589(7840):70–75

Abernathey RP, Cerovecki I, Holland PR, Newsom E, Mazloff M, Talley LD. 2016. Water-mass transformation by sea ice in the upper branch of the Southern Ocean overturning. *Nat. Geosci.* 9(8):596–601

Ai XE, Studer AS, Sigman DM, Martínez-García A, Fripiat F, et al. 2020. Southern Ocean upwelling, Earth's obliquity, and glacial-interglacial atmospheric CO_2 change. *Science* 370(6522):1348–52

Amante C, Eakins BW. 2009. *ETOPO1 1 Arc-Minute Global Relief Model: procedures, data sources and analysis.* Tech. Memo. NESDIS NGDC-24, Natl. Geophys. Data Cent., Natl. Ocean. Atmos. Adm., Boulder, CO. **https://doi.org/10.7289/V5C8276M**

Arroyo MC, Shadwick EH, Tilbrook B, Rintoul SR, Kusahara K. 2020. A continental shelf pump for CO_2 on the Adélie Land coast, East Antarctica. *J. Geophys. Res. Oceans* 125(10):e2020JC016302

Arteaga LA, Boss E, Behrenfeld MJ, Westberry TK, Sarmiento JL. 2020. Seasonal modulation of phytoplankton biomass in the Southern Ocean. *Nat. Commun.* 11:5364

Arteaga LA, Pahlow M, Bushinsky SM, Sarmiento JL. 2019. Nutrient controls on export production in the Southern Ocean. *Glob. Biogeochem. Cycles* 33(8):942–56

Bachman SD, Taylor JR, Adams KA, Hosegood PJ. 2017. Mesoscale and submesoscale effects on mixed layer depth in the Southern Ocean. *J. Phys. Oceanogr.* 47(9):2173–88

Bakker DC, Pfeil B, Landa CS, Metzl N, O'Brien KM, et al. 2016. A multi-decade record of high-quality fCO_2 data in version 3 of the Surface Ocean CO_2 Atlas (SOCAT). *Earth Syst. Sci. Data* 8(2):383–413

Balwada D, Gray AR, Dove LA, Thompson AF. 2023. Tracer stirring and variability in the Antarctic Circumpolar Current near the Southwest Indian Ridge. ESS Open Arch. 167839945.50522830. **https://doi.org/10.22541/essoar.167839945.50522830/v1**

Balwada D, Smith KS, Abernathey R. 2018. Submesoscale vertical velocities enhance tracer subduction in an idealized Antarctic Circumpolar Current. *Geophys. Res. Lett.* 45(18):9790–802

Bittig HC, Steinhoff T, Claustre H, Fiedler B, Williams NL, et al. 2018. An alternative to static climatologies: robust estimation of open ocean CO_2 variables and nutrient concentrations from T, S, and O_2 data using Bayesian neural networks. *Front. Mar. Sci.* 5:328

Boutin J, Merlivat L, Henocq C, Martin N, Sallée JB. 2008. Air–sea CO_2 flux variability in frontal regions of the Southern Ocean from CARbon Interface OCean Atmosphere drifters. *Limnol. Oceanogr.* 53(5, part 2):2062–79

Brand SVS, Prend CJ, Talley LD. 2023. Modification of North Atlantic Deep Water by Pacific/Upper Circumpolar Deep Water in the Argentine Basin. *Geophys. Res. Lett.* 50(2):e2022GL099419

Busecke JJ, Abernathey RP. 2019. Ocean mesoscale mixing linked to climate variability. *Sci. Adv.* 5(1):eaav5014

Bushinsky SM, Cerovečki I. 2023. Subantarctic mode water biogeochemical formation properties and interannual variability. *AGU Adv.* 4(2):e2022AV000722

Bushinsky SM, Landschützer P, Rödenbeck C, Gray AR, Baker D, et al. 2019a. Reassessing Southern Ocean air-sea CO_2 flux estimates with the addition of biogeochemical float observations. *Glob. Biogeochem. Cycles* 33(11):1370–88

Bushinsky SM, Takeshita Y, Williams NL. 2019b. Observing changes in ocean carbonate chemistry: our autonomous future. *Curr. Clim. Change Rep.* 5(3):207–20

Byrne D, Münnich M, Frenger I, Gruber N. 2016. Mesoscale atmosphere ocean coupling enhances the transfer of wind energy into the ocean. *Nat. Commun.* 7:ncomms11867

Cai Y, Chen D, Mazloff MR, Lian T, Liu X. 2022. Topographic modulation of the wind stress impact on eddy activity in the Southern Ocean. *Geophys. Res. Lett.* 49(13):e2022GL097859

Carranza MM, Gille ST, Franks PJS, Johnson KS, Pinkel R, Girton JB. 2018. When mixed layers are not mixed. Storm-driven mixing and bio-optical vertical gradients in mixed layers of the Southern Ocean. *J. Geophys. Res. Oceans* 123(10):7264–89

Carroll D, Menemenlis D, Adkins JF, Bowman KW, Brix H, et al. 2020. The ECCO-Darwin data-assimilative global ocean biogeochemistry model: estimates of seasonal to multidecadal surface ocean pCO_2 and air-sea CO_2 flux. *J. Adv. Model. Earth Syst.* 12(10):e2019MS001888

Chen H, Haumann FA, Talley LD, Johnson KS, Sarmiento JL. 2022. The deep ocean's carbon exhaust. *Glob. Biogeochem. Cycles* 36(7):e2021GB007156

Chikamoto MO, DiNezio P. 2021. Multi-century changes in the ocean carbon cycle controlled by the tropical oceans and the Southern Ocean. *Glob. Biogeochem. Cycles* 35(12):e2021GB007090

Clement D, Gruber N. 2018. The eMLR(C*) method to determine decadal changes in the global ocean storage of anthropogenic CO_2. *Glob. Biogeochem. Cycles* 32(4):654–79

Coggins A, Watson AJ, Schuster U, Mackay N, King B, et al. 2023. Surface ocean carbon budget in the 2017 south Georgia diatom bloom: observations and validation of profiling Biogeochemical Argo floats. *Deep-Sea Res. II* 209:105275

Davila X, Gebbie G, Brakstad A, Lauvset SK, McDonagh EL, et al. 2022. How is the ocean anthropogenic carbon reservoir filled? *Glob. Biogeochem. Cycles* 36(5):e2021GB007055

Dawson HRS, Strutton PG, Gaube P. 2018. The unusual surface chlorophyll signatures of Southern Ocean eddies. *J. Geophys. Res. Oceans* 123(9):6053–69

Deacon GER. 1937. *The Hydrology of the Southern Ocean*. Discov. Rep. Vol. 15. Cambridge, UK: Cambridge Univ. Press

Deike L. 2022. Mass transfer at the ocean–atmosphere interface: the role of wave breaking, droplets, and bubbles. *Annu. Rev. Fluid Mech.* 54:191–224
Della Penna A, Llort J, Moreau S, Patel R, Kloser R, et al. 2022. The impact of a Southern Ocean cyclonic eddy on mesopelagic micronekton. *J. Geophys. Res. Oceans* 127(11):e2022JC018893
Della Penna A, Trull TW, Wotherspoon S, De Monte S, Johnson CR, d'Ovidio F. 2018. Mesoscale variability of conditions favoring an iron-induced diatom bloom downstream of the Kerguelen Plateau. *J. Geophys. Res. Oceans* 123(5):3355–67
DeVries T. 2014. The oceanic anthropogenic CO_2 sink: storage, air-sea fluxes, and transports over the industrial era. *Glob. Biogeochem. Cycles* 28(7):631–47
DeVries T. 2022. Atmospheric CO_2 and sea surface temperature variability cannot explain recent decadal variability of the ocean CO_2 sink. *Geophys. Res. Lett.* 49(7):e2021GL096018
Dickson A. 2010. The carbon dioxide system in seawater: equilibrium chemistry and measurements. In *Guide to Best Practices for Ocean Acidification Research and Data Reporting*, ed. U Riebesell, VJ Fabry, L Hansson, J-P Gattuso, pp. 17–40. Luxembourg: Publ. Off. Eur. Union
Djeutchouang LM, Chang N, Gregor L, Vichi M, Monteiro PMS. 2022. The sensitivity of pCO_2 reconstructions to sampling scales across a Southern Ocean sub-domain: a semi-idealized ocean sampling simulation approach. *Biogeosciences* 19(17):4171–95
Dove LA, Balwada D, Thompson AF, Gray AR. 2022. Enhanced ventilation in energetic regions of the Antarctic Circumpolar Current. *Geophys. Res. Lett.* 49(13):e2021GL097574
Dove LA, Thompson AF, Balwada D, Gray AR. 2021. Observational evidence of ventilation hotspots in the Southern Ocean. *J. Geophys. Res. Oceans* 126(7):e2021JC017178
Dove LA, Viglione GA, Thompson AF, Flexas MM, Cason TR, Sprintall J. 2023. Controls on wintertime ventilation in southern Drake Passage. *Geophys. Res. Lett.* 50(5):e2022GL102550
du Plessis MD, Swart S, Biddle LC, Giddy IS, Monteiro PMS, et al. 2022. The daily-resolved Southern Ocean mixed layer: regional contrasts assessed using glider observations. *J. Geophys. Res. Oceans* 127(4):e2021JC017760
Dufour CO, Griffies SM, de Souza GF, Frenger I, Morrison AK, et al. 2015. Role of mesoscale eddies in cross-frontal transport of heat and biogeochemical tracers in the Southern Ocean. *J. Phys. Oceanogr.* 45(12):3057–81
Ellwood MJ, Strzepek RF, Strutton PG, Trull TW, Fourquez M, Boyd PW. 2020. Distinct iron cycling in a Southern Ocean eddy. *Nat. Commun.* 11:825
Fairall CW, Yang M, Brumer SE, Blomquist BW, Edson JB, et al. 2022. Air-sea trace gas fluxes: direct and indirect measurements. *Front. Mar. Sci.* 9:1043
Fernández Castro B, Mazloff M, Williams RG, Naveira Garabato AC. 2022. Subtropical contribution to Sub-Antarctic Mode Waters. *Geophys. Res. Lett.* 49(11):e2021GL097560
Fogt RL, Jones JM, Renwick J. 2012. Seasonal zonal asymmetries in the Southern Annular Mode and their impact on regional temperature anomalies. *J. Clim.* 25(18):6253–70
Frölicher TL, Sarmiento JL, Paynter DJ, Dunne JP, Krasting JP, Winton M. 2015. Dominance of the Southern Ocean in anthropogenic carbon and heat uptake in CMIP5 models. *J. Clim.* 28(2):862–86
Gallego MA, Timmermann A, Friedrich T, Zeebe RE. 2020. Anthropogenic intensification of surface ocean interannual pCO_2 variability. *Geophys. Res. Lett.* 47:e2020GL087104
Garabato AC, MacGilchrist GA, Brown PJ, Evans DG, Meijers AJ, Zika JD. 2017. High-latitude ocean ventilation and its role in Earth's climate transitions. *Philos. Trans. R. Soc. A* 375(2102):20160324
Gille ST, Sheen KL, Swart S, Thompson AF. 2022. Mixing in the Southern Ocean. In *Ocean Mixing: Drivers, Mechanisms and Impacts*, ed. M Meredith, A Naveira Garabato, pp. 301–27. Amsterdam: Elsevier
Gloege L, McKinley GA, Landschützer P, Fay AR, Frölicher TL, et al. 2021. Quantifying errors in observationally based estimates of ocean carbon sink variability. *Glob. Biogeochem. Cycles* 35(4):e2020GB006788
Gloege L, Yan M, Zheng T, McKinley GA. 2022. Improved quantification of ocean carbon uptake by using machine learning to merge global models and pCO_2 data. *J. Adv. Model. Earth Syst.* 14(2):e2021MS002620
Gray AR, Johnson KS, Bushinsky SM, Riser SC, Russell JL, et al. 2018. Autonomous biogeochemical floats detect significant carbon dioxide outgassing in the high-latitude Southern Ocean. *Geophys. Res. Lett.* 45(17):9049–57

Gregor L, Gruber N. 2021. OceanSODA-ETHZ: a global gridded data set of the surface ocean carbonate system for seasonal to decadal studies of ocean acidification. *Earth Syst. Sci. Data* 13(2):777–808

Gregor L, Lebehot AD, Kok S, Scheel Monteiro PM. 2019. A comparative assessment of the uncertainties of global surface ocean CO_2 estimates using a machine-learning ensemble (CSIR-ML6 version 2019a) – have we hit the wall? *Geosci. Model Dev.* 12(12):5113–36

Gruber N, Bakker DC, DeVries T, Gregor L, Hauck J, et al. 2023. Trends and variability in the ocean carbon sink. *Nat. Rev. Earth Environ.* 4(2):119–34

Gruber N, Clement D, Carter BR, Feely RA, van Heuven, et al. 2019a. The oceanic sink for anthropogenic CO_2 from 1994 to 2007. *Science* 363(6432):1193–99

Gruber N, Landschützer P, Lovenduski NS. 2019b. The variable Southern Ocean carbon sink. *Annu. Rev. Mar. Sci.* 11:159–86

Harrison CS, Long MC, Lovenduski NS, Moore JK. 2018. Mesoscale effects on carbon export: a global perspective. *Glob. Biogeochem. Cycles* 32(4):680–703

Hauck J, Zeising M, Le Quéré C, Gruber N, Bakker DCE, et al. 2020. Consistency and challenges in the ocean carbon sink estimate for the global carbon budget. *Front. Mar. Sci.* 7:571720

Haumann FA, Gruber N, Münnich M, Frenger I, Kern S. 2016. Sea-ice transport driving Southern Ocean salinity and its recent trends. *Nature* 537(7618):89–92

Hausmann U, McGillicuddy DJ Jr., Marshall J. 2017. Observed mesoscale eddy signatures in Southern Ocean surface mixed-layer depth. *J. Geophys. Res. Oceans* 122(1):617–35

Hersbach H, Bell B, Berrisford P, Biavati G, Horányi A, et al. 2023. *ERA5 monthly averaged data on single levels from 1940 to present*. Dataset, Copernic. Clim. Change Serv. (C3S) Clim. Data Store (CDS). **https://doi.org/10.24381/cds.f17050d7**

Holzer M, DeVries T. 2022. Source-labeled anthropogenic carbon reveals a large shift of preindustrial carbon from the ocean to the atmosphere. *Glob. Biogeochem. Cycles* 36(10):e2022GB007405

Hoskins BJ, Hodges KI. 2005. A new perspective on Southern Hemisphere storm tracks. *J. Clim.* 18(20):4108–29

Inatsu M, Hoskins BJ. 2004. The zonal asymmetry of the Southern Hemisphere winter storm track. *J. Clim.* 17(24):4882–92

Iudicone D, Rodgers KB, Plancherel Y, Aumont O, Ito T, et al. 2016. The formation of the ocean's anthropogenic carbon reservoir. *Sci. Rep.* 6:35473

Iversen MH. 2023. Carbon export in the ocean: a biologist's perspective. *Annu. Rev. Mar. Sci.* 15:357–81

Jersild A, Delawalla S, Ito T. 2021. Mesoscale eddies regulate seasonal iron supply and carbon drawdown in the Drake Passage. *Geophys. Res. Lett.* 48(24)

Johnson GC, Hosoda S, Jayne SR, Oke PR, Riser SC, et al. 2022. Argo—two decades: global oceanography, revolutionized. *Annu. Rev. Mar. Sci.* 14:379–403

Johnson GC, Lyman JM. 2022. GOSML: a global ocean surface mixed layer statistical monthly climatology: means, percentiles, skewness, and kurtosis. *J. Geophys. Res. Oceans* 127(1):e2021JC018219

Jones EM, Hoppema M, Strass V, Hauck J, Salt L, et al. 2017. Mesoscale features create hotspots of carbon uptake in the Antarctic Circumpolar Current. *Deep-Sea Res. II* 138:39–51

Joy-Warren HL, Dijken GL, Alderkamp A, Leventer A, Lewis KM, et al. 2019. Light is the primary driver of early season phytoplankton production along the western Antarctic Peninsula. *J. Geophys. Res. Oceans* 124(11):7375–99

Keppler L, Landschützer P. 2019. Regional wind variability modulates the Southern Ocean carbon sink. *Sci. Rep.* 9:7384

Keppler L, Landschützer P, Gruber N, Lauvset SK, Stemmler I. 2020. Seasonal carbon dynamics in the near-global ocean. *Glob. Biogeochem. Cycles* 34(12):e2020GB006571

Key RM, Olsen A, van Heuven S, Lauvset SK, Velo A, et al. 2015. *Global Ocean Data Analysis Project, version 2 (GLODAPv2)*. Rep. ORNL/CDIAC-162, NDP-093, Carbon Dioxide Inf. Anal. Cent., Oak Ridge Natl. Lab., Oak Ridge, TN

Kim YS, Orsi AH. 2014. On the variability of Antarctic Circumpolar Current fronts inferred from 1992–2011 altimetry. *J. Phys. Oceanogr.* 44(12):3054–71

Krumhardt KM, Long MC, Lindsay K, Levy MN. 2020. Southern Ocean calcification controls the global distribution of alkalinity. *Glob. Biogeochem. Cycles* 34(12):e2020GB006727

Landschützer P, Bushinsky S, Gray AR. 2019a. *A combined globally mapped CO_2 flux estimate based on the Surface Ocean CO_2 Atlas Database (SOCAT) and Southern Ocean Carbon and Climate Observations and Modeling (SOCCOM) biogeochemistry floats from 1982 to 2017 (NCEI Accession 0191304)*. Dataset Version 2.2, Natl. Cent. Environ. Inf., Natl. Ocean. Atmos. Adm. **https://doi.org/10.25921/9hsn-xq82**

Landschützer P, Gruber N, Bakker DCE. 2016. Decadal variations and trends of the global ocean carbon sink. *Glob. Biogeochem. Cycles* 30(10):1396–417

Landschützer P, Gruber N, Bakker DCE. 2021. *An observation-based global monthly gridded sea surface p CO_2 product from 1982 onward and its monthly climatology (NCEI Accession 0160558)*. Dataset Version 5.5, Natl. Cent. Environ. Inf., Natl. Ocean. Atmos. Adm. **https://doi.org/10.7289/v5z899n6**

Landschützer P, Gruber N, Haumann FA, Rödenbeck C, Bakker DCE, et al. 2015. The reinvigoration of the Southern Ocean carbon sink. *Science* 349(6253):1221–24

Landschützer P, Ilyina T, Lovenduski NS. 2019b. Detecting regional modes of variability in observation-based surface ocean pCO_2. *Geophys. Res. Lett.* 46(5):2670–79

Lauvset SK, Key RM, Olsen A, van Heuven S, Velo A, et al. 2016. A new global interior ocean mapped climatology: the 1° × 1° GLODAP version 2. *Earth Syst. Sci. Data* 8(2):325–40

Le Quéré C, Rodenbeck C, Buitenhuis ET, Conway TJ, Langenfelds R, et al. 2007. Saturation of the Southern Ocean CO_2 sink due to recent climate change. *Science* 316(5832):1735–38

Lévy M, Resplandy L, Lengaigne M. 2014. Oceanic mesoscale turbulence drives large biogeochemical interannual variability at middle and high latitudes. *Geophys. Res. Lett.* 41(7):2467–74

Li H, Ilyina T. 2018. Current and future decadal trends in the oceanic carbon uptake are dominated by internal variability. *Geophys. Res. Lett.* 45:916–25

Llort J, Langlais C, Matear R, Moreau S, Lenton A, Strutton PG. 2018. Evaluating Southern Ocean carbon eddy-pump from Biogeochemical-Argo floats. *J. Geophys. Res. Oceans* 123(2):971–84

Long MC, Stephens BB, McKain K, Sweeney C, Keeling RF, et al. 2021. Strong Southern Ocean carbon uptake evident in airborne observations. *Science* 374(6572):1275–80

MacGilchrist GA, Naveira Garabato AC, Brown PJ, Jullion L, Bacon S, et al. 2019. Reframing the carbon cycle of the subpolar Southern Ocean. *Sci. Adv.* 5(8):eaav6410

Marshall D. 1995. Topographic steering of the Antarctic Circumpolar Current. *J. Phys. Oceanogr.* 25(7):1636–50

Marshall J, Speer K. 2012. Closure of the meridional overturning circulation through Southern Ocean upwelling. *Nat. Geosci.* 5(3):171–80

McKinley GA, Fay AR, Eddebbar YA, Gloege L, Lovenduski NS. 2020. External forcing explains recent decadal variability of the ocean carbon sink. *AGU Adv.* 1(2):e2019AV000149

Meier WN, Fetterer F, Windnagel AK, Stewart JS. 2021. *NOAA/NSIDC climate data record of passive microwave sea ice concentration, version 4*. Dataset G02202, Natl. Snow Ice Data Cent. **https://doi.org/10.7265/efmz-2t65**

Mongwe NP, Vichi M, Monteiro PMS. 2018. The seasonal cycle of pCO_2 and CO_2 fluxes in the Southern Ocean: diagnosing anomalies in CMIP5 Earth system models. *Biogeosciences* 15(9):2851–72

Moreau S, Della Penna A, Llort J, Patel R, Langlais C, et al. 2017. Eddy-induced carbon transport across the Antarctic Circumpolar Current. *Glob. Biogeochem. Cycles* 31(9):1368–86

Morrison AK, Frölicher TL, Sarmiento JL. 2014. Upwelling in the Southern Ocean. *Phys. Today* 68(1):27–32

Morrison AK, Waugh DW, Hogg AM, Jones DC, Abernathey RP. 2022. Ventilation of the Southern Ocean pycnocline. *Annu. Rev. Mar. Sci.* 14:405–30

Munday DR, Johnson HL, Marshall DP. 2014. Impacts and effects of mesoscale ocean eddies on ocean carbon storage and atmospheric pCO_2. *Glob. Biogeochem. Cycles* 28(8):877–96

Munk WH, Palmén E. 1951. Note on the dynamics of the Antarctic Circumpolar Current. *Tellus* 3(1):53–55

NASA Ocean Biol. Process. Group. 2022. *Moderate-resolution Imaging Spectroradiometer (MODIS) Aqua Level-3 Mapped Chlorophyll Data, version R2022*. Dataset, NASA Ocean Biol. Distrib. Active Arch. Cent.

Nevison CD, Munro DR, Lovenduski NS, Keeling RF, Manizza M, et al. 2020. Southern Annular Mode influence on wintertime ventilation of the Southern Ocean detected in atmospheric O_2 and CO_2 measurements. *Geophys. Res. Lett.* 47(4):e2019GL085667

Nicholson SA, Lévy M, Jouanno J, Capet X, Swart S, Monteiro PMS. 2019. Iron supply pathways between the surface and subsurface waters of the Southern Ocean: from winter entrainment to summer storms. *Geophys. Res. Lett.* 46(24):14567–75

Nicholson SA, Whitt DB, Fer I, du Plessis MD, Lebéhot AD, et al. 2022. Storms drive outgassing of CO_2 in the subpolar Southern Ocean. *Nat. Commun.* 13:158

Noh KM, Lim HG, Kug JS. 2021. Zonally asymmetric phytoplankton response to the Southern Annular Mode in the marginal sea of the Southern Ocean. *Sci. Rep.* 11:10266

Nowlin WD, Klinck JM. 1986. The physics of the Antarctic Circumpolar Current. *Rev. Geophys.* 24(3):469–91

Ohshima KI, Nihashi S, Iwamoto K. 2016. Global view of sea-ice production in polynyas and its linkage to dense/bottom water formation. *Geosci. Lett.* 3:13

Olsen A, Key RM, van Heuven S, Lauvset SK, Velo A, et al. 2016. The Global Ocean Data Analysis Project version 2 (GLODAPv2) – an internally consistent data product for the world ocean. *Earth Syst. Sci. Data* 8(2):297–323

Orsi AH, Whitworth T, Nowlin WD. 1995. On the meridional extent and fronts of the Antarctic Circumpolar Current. *Deep-Sea Res. I* 42(5):641–73

Patel RS, Llort J, Strutton PG, Phillips HE, Moreau S, et al. 2020. The biogeochemical structure of Southern Ocean mesoscale eddies. *J. Geophys. Res. Oceans* 125(8):e2020JC016115

Person R, Aumont O, Lévy M. 2018. The biological pump and seasonal variability of pCO_2 in the Southern Ocean: exploring the role of diatom adaptation to low iron. *J. Geophys. Res. Oceans* 123(5):3204–26

Pezzi LP, de Souza RB, Santini MF, Miller AJ, Carvalho JT, et al. 2021. Oceanic eddy-induced modifications to air–sea heat and CO_2 fluxes in the Brazil-Malvinas Confluence. *Sci. Rep.* 11:10648

Prend CJ, Gray AR, Talley LD, Gille ST, Haumann FA, et al. 2022a. Indo-Pacific sector dominates Southern Ocean carbon outgassing. *Glob. Biogeochem. Cycles* 36(7):e2021GB007226

Prend CJ, Hunt JM, Mazloff MR, Gille ST, Talley LD. 2022b. Controls on the boundary between thermally and non-thermally driven pCO_2 regimes in the South Pacific. *Geophys. Res. Lett.* 49(9):e2021GL095797

Prend CJ, Keerthi MG, Lévy M, Aumont O, Gille ST, Talley LD. 2022c. Sub-seasonal forcing drives year-to-year variations of Southern Ocean primary productivity. *Glob. Biogeochem. Cycles* 36(7):e2022GB007329

Priestley MD, Ackerley D, Catto JL, Hodges KI, McDonald RE, Lee RW. 2020. An overview of the extratropical storm tracks in CMIP6 historical simulations. *J. Clim.* 33(15):6315–43

Rae JWB, Burke A, Robinson LF, Adkins JF, Chen T, et al. 2018. CO_2 storage and release in the deep Southern Ocean on millennial to centennial timescales. *Nature* 562(7728):569–73

Resplandy L, Boutin J, Merlivat L. 2014. Observed small spatial scale and seasonal variability of the CO_2 system in the Southern Ocean. *Biogeosciences* 11(1):75–90

Resplandy L, Keeling RF, Rödenbeck C, Stephens BB, Khatiwala S, et al. 2018. Revision of global carbon fluxes based on a reassessment of oceanic and riverine carbon transport. *Nat. Geosci.* 11(7):504–9

Rintoul SR. 2018. The global influence of localized dynamics in the Southern Ocean. *Nature* 558(7709):209–18

Risien CM, Chelton DB. 2008. A global climatology of surface wind and wind stress fields from eight years of QuikSCAT scatterometer data. *J. Phys. Oceanogr.* 38:2379–413

Rödenbeck C, Bakker DC, Metzl N, Olsen A, Sabine C, et al. 2014. Interannual sea-air CO_2 flux variability from an observation-driven ocean mixed-layer scheme. *Biogeosciences* 11(17):4599–613

Rödenbeck C, DeVries T, Hauck J, Le Quéré C, Keeling RF. 2022. Data-based estimates of interannual sea–air CO_2 flux variations 1957–2020 and their relation to environmental drivers. *Biogeosciences* 19(10):2627–52

Sallée JB, Matear RJ, Rintoul SR, Lenton A. 2012. Localized subduction of anthropogenic carbon dioxide in the Southern Hemisphere oceans. *Nat. Geosci.* 5(8):579–84

Sallée JB, Speer KG, Rintoul SR. 2010. Zonally asymmetric response of the Southern Ocean mixed-layer depth to the Southern Annular Mode. *Nat. Geosci.* 3(4):273–79

Sallée JB, Speer KG, Rintoul SR. 2011. Mean-flow and topographic control on surface eddy-mixing in the Southern Ocean. *J. Mar. Res.* 69(4):753–77

Sarmiento JL, Gruber N. 2006. *Ocean Biogeochemical Dynamics*. Princeton, NJ: Princeton Univ. Press

Sarmiento JL, Gruber N, Brzezinski MA, Dunne JP. 2004. High-latitude controls of thermocline nutrients and low latitude biological productivity. *Nature* 427(6969):56–60

Sarmiento JL, Johnson KS, Arteaga LA, Bushinsky SM, Cullen HM, et al. 2023. The Southern Ocean Carbon and Climate Observations and Modeling (SOCCOM) project: a review. *Prog. Oceanogr.* 219:103130

Schroeter S, O'Kane TJ, Sandery PA. 2023. Antarctic sea ice regime shift associated with decreasing zonal symmetry in the Southern Annular Mode. *Cryosphere* 17(2):701–17

Shadwick EH, Trull TW, Tilbrook B, Sutton AJ, Schulz E, Sabine CL. 2015. Seasonality of biological and physical controls on surface ocean CO_2 from hourly observations at the Southern Ocean Time Series site south of Australia. *Glob. Biogeochem. Cycles* 29(2):223–38

Siegel DA, DeVries T, Cetinić I, Bisson KM. 2023. Quantifying the ocean's biological pump and its carbon cycle impacts on global scales. *Annu. Rev. Mar. Sci.* 15:329–56

Smith KM, Hamlington PE, Niemeyer KE, Fox-Kemper B, Lovenduski NS. 2018. Effects of Langmuir turbulence on upper ocean carbonate chemistry. *J. Adv. Model. Earth Syst.* 10(12):3030–48

Song H, Marshall J, Campin J, McGillicuddy DJ Jr. 2019. Impact of near-inertial waves on vertical mixing and air-sea CO_2 fluxes in the Southern Ocean. *J. Geophys. Res. Oceans* 124(7):4605–17

Song H, Marshall J, McGillicuddy DJ Jr., Seo H. 2020. Impact of current-wind interaction on vertical processes in the Southern Ocean. *J. Geophys. Res. Oceans* 125(4):e2020JC016046

Song H, Marshall J, Munro DR, Dutkiewicz S, Sweeney C, et al. 2016. Mesoscale modulation of air-sea CO_2 flux in Drake Passage. *J. Geophys. Res. Oceans* 121(9):6635–49

Studer AS, Sigman DM, Martínez-García A, Thöle LM, Michel E, et al. 2018. Increased nutrient supply to the Southern Ocean during the Holocene and its implications for the pre-industrial atmospheric CO_2 rise. *Nat. Geosci.* 11(10):756–60

Stukel MR, Ducklow HW. 2017. Stirring up the biological pump: vertical mixing and carbon export in the Southern Ocean. *Glob. Biogeochem. Cycles* 31(9):1420–34

Su Z, Wang J, Klein P, Thompson AF, Menemenlis D. 2018. Ocean submesoscales as a key component of the global heat budget. *Nat. Commun.* 9:775

Sutton AJ, Williams NL, Tilbrook B. 2021. Constraining Southern Ocean CO_2 flux uncertainty using uncrewed surface vehicle observations. *Geophys. Res. Lett.* 48(3):e2020GL091748

Swart S, Gille ST, Delille B, Josey S, Mazloff M, et al. 2019. Constraining Southern Ocean air-sea-ice fluxes through enhanced observations. *Front. Mar. Sci.* 6:421

Tagliabue A, Sallée JB, Bowie AR, Lévy M, Swart S, Boyd PW. 2014. Surface-water iron supplies in the Southern Ocean sustained by deep winter mixing. *Nat. Geosci.* 7(4):314–20

Tak YJ, Song H, Noh Y, Choi Y. 2023. Physical and biogeochemical responses in the Southern Ocean to a simple parameterization of Langmuir circulation. *Ocean Model.* 181:102152

Takahashi T, Olafsson J, Goddard JG, Chipman DW, Sutherland SC. 1993. Seasonal variation of CO_2 and nutrients in the high-latitude surface oceans: a comparative study. *Glob. Biogeochem. Cycles* 7(4):843–78

Takahashi T, Sutherland SC, Sweeney C, Poisson A, Metzl N, et al. 2002. Global sea–air CO_2 flux based on climatological surface ocean pCO_2, and seasonal biological and temperature effects. *Deep-Sea Res. II* 49(9–10):1601–22

Talley L. 2013. Closure of the global overturning circulation through the Indian, Pacific, and Southern Oceans: schematics and transports. *Oceanography* 26(1):80–97

Talley L, Feely R, Sloyan B, Wanninkhof R, Baringer M, et al. 2016. Changes in ocean heat, carbon content, and ventilation: a review of the first decade of GO-SHIP global repeat hydrography. *Annu. Rev. Mar. Sci.* 8:185–215

Tamsitt V, Drake HF, Morrison AK, Talley LD, Dufour CO, et al. 2017. Spiraling pathways of global deep waters to the surface of the Southern Ocean. *Nat. Commun.* 8:172

Tamsitt V, Talley LD, Mazloff MR, Cerovečki I. 2016. Zonal variations in the Southern Ocean heat budget. *J. Clim.* 29(18):6563–79

Taylor JR, Bachman S, Stamper M, Hosegood P, Adams K, et al. 2018. Submesoscale Rossby waves on the Antarctic circumpolar current. *Sci. Adv.* 4(3):eaao2824

Taylor JR, Thompson AF. 2023. Submesoscale dynamics in the upper ocean. *Annu. Rev. Fluid Mech.* 55:103–27

Thompson AF, Sallée JB. 2012. Jets and topography: jet transitions and the impact on transport in the Antarctic Circumpolar Current. *J. Phys. Oceanogr.* 42(6):956–72

Tréguer P, Bowler C, Moriceau B, Dutkiewicz S, Gehlen M, et al. 2018. Influence of diatom diversity on the ocean biological carbon pump. *Nat. Geosci.* 11:27–37

Uchida T, Balwada D, Abernathey RP, McKinley GA, Smith SK, Lévy M. 2019. The contribution of submesoscale over mesoscale eddy iron transport in the open Southern Ocean. *J. Adv. Model. Earth Syst.* 11(12):3934–58

Uchida T, Balwada D, Abernathey RP, McKinley GA, Smith SK, Lévy M. 2020. Vertical eddy iron fluxes support primary production in the open Southern Ocean. *Nat. Commun.* 11:1125

Verdy A, Mazloff MR. 2017. A data assimilating model for estimating Southern Ocean biogeochemistry. *J. Geophys. Res. Oceans* 122(9):6968–88

Viglione GA, Thompson AF. 2016. Lagrangian pathways of upwelling in the Southern Ocean. *J. Geophys. Res. Oceans* 121(8):6295–309

Wanninkhof R, Asher WE, Ho DT, Sweeney C, McGillis WR. 2009. Advances in quantifying air-sea gas exchange and environmental forcing. *Annu. Rev. Mar. Sci.* 1:213–44

Watson AJ, Ledwell JR, Messias MJ, King BA, Mackay N, et al. 2013. Rapid cross-density ocean mixing at mid-depths in the Drake Passage measured by tracer release. *Nature* 501(7467):408–11

Watts J, Bell TG, Anderson K, Butterworth BJ, Miller S, et al. 2022. Impact of sea ice on air-sea CO_2 exchange – a critical review of polar eddy covariance studies. *Prog. Oceanogr.* 201:102741

Williams NL, Juranek LW, Feely RA, Johnson KS, Sarmiento JL, et al. 2017. Calculating surface ocean pCO_2 from Biogeochemical Argo floats equipped with pH: an uncertainty analysis. *Glob. Biogeochem. Cycles* 31(3):591–604

Williams RG, Follows MJ. 2011. *Ocean Dynamics and the Carbon Cycle: Principles and Mechanisms*. Cambridge, UK: Cambridge Univ. Press

Woolf DK, Shutler JD, Goddijn-Murphy L, Watson AJ, Chapron B, et al. 2019. Key uncertainties in the recent air-sea flux of CO_2. *Glob. Biogeochem. Cycles* 33(12):1548–63

Wu Y, Hain MP, Humphreys MP, Hartman S, Tyrrell T. 2019. What drives the latitudinal gradient in open-ocean surface dissolved inorganic carbon concentration? *Biogeosciences* 16(13):2661–81

Yang B, Shadwick EH, Schultz C, Doney SC. 2021. Annual mixed layer carbon budget for the West Antarctic Peninsula continental shelf: insights from year-round mooring measurements. *J. Geophys. Res. Oceans* 126(4):e2020JC016920

Yang M, Bell TG, Bidlot JR, Blomquist BW, Butterworth BJ, et al. 2022. Global synthesis of air-sea CO_2 transfer velocity estimates from ship-based eddy covariance measurements. *Front. Mar. Sci.* 9:1107

Yang M, Smyth TJ, Kitidis V, Brown IJ, Wohl C, et al. 2021. Natural variability in air–sea gas transfer efficiency of CO_2. *Sci. Rep.* 11:13584

Young IR, Fontaine E, Liu Q, Babanin AV. 2020. The wave climate of the Southern Ocean. *J. Phys. Oceanogr.* 50(5):1417–33

Yung CK, Morrison AK, Hogg AMC. 2022. Topographic hotspots of Southern Ocean eddy upwelling. *Front. Mar. Sci.* 9:769

Zemskova VE, He TL, Wan Z, Grisouard N. 2022. A deep-learning estimate of the decadal trends in the Southern Ocean carbon storage. *Nat. Commun.* 13:4056

Zhang Z, Liu Y, Qiu B, Luo Y, Cai W, et al. 2023. Submesoscale inverse energy cascade enhances Southern Ocean eddy heat transport. *Nat. Commun.* 14:1335

Zilberman NV, Scanderbeg M, Gray AR, Oke PR. 2023. Scripps Argo trajectory-based velocity product: global estimates of absolute velocity derived from Core, Biogeochemical, and Deep Argo float trajectories at parking depth. *J. Atmos. Ocean. Technol.* 40(3):361–74